Arch Gynecol Obstet (2014) 289:1061–1069
DOI 10.1007/s00404-013-3060-0

GYNECOLOGIC ONCOLOGY

Epigenetic and expression analysis of *TRAIL-R2* and *BCL2*: on the TRAIL to knowledge of apoptosis in ovarian tumors

Letícia da Conceição Braga · Luciana Maria Silva · Josiane Barbosa Piedade · Paulo Traiman · Agnaldo Lopes da Silva Filho

Received: 27 March 2013 / Accepted: 15 October 2013 / Published online: 5 November 2013

Abstract
Objective This study assesses *TRAIL-R2 (*TNF-related apoptosis-inducing ligand receptor 2) and *BCL2* (B cell CLL/lymphoma 2) expression as well as CpG island methylation within the *TRAIL-R2* promoter in ovarian serous tumors and primary and metastatic serous EOC (epithelial ovarian cancer).
Methods RNA and DNA were obtained from women with normal ovarian tissues ($n = 18$), ovarian serous cystadenoma tumors ($n = 11$) and serous EOC ($n = 16$) using Trizol®. Quantitative PCR was performed to quantify the relative levels of *TRAIL-R2* and *BCL2*. The methylation frequency of the *TRAIL-R3* promoter was assessed using a methylation-specific PCR assay after DNA bisulfite conversion. Differences between the groups were evaluated using the χ^2, Mann–Whitney *U* or Kruskal–Wallis tests, as indicated.
Results We identified *TRAIL-R2* and *BCL2* mRNA expressed in all ovarian tumor groups, and there were significant differences between the groups. Both genes had low expression levels in ovarian serous cystadenoma and primary EOC tumors when compared with metastatic EOC. Methylation of the *TRAIL-R2* promoter was frequently observed in all groups; however, there were no statistically significant associations.
Conclusions Primary EOC is associated with lower *TRAIL-R2* and *BCL2* expression levels, while metastatic EOC is associated with higher expression of these genes. Promoter DNA methylation was not related to this finding, suggesting there are other mechanisms involved in transcriptional control.

Keywords Ovarian tumors · *TRAIL-R2* · *BCL2* · Gene expression · DNA methylation

Introduction

Apoptotic cell death can be triggered by two alternative, convergent pathways: the extrinsic pathway, which is mediated by the activation of membrane-bound death receptors (DRs), and the intrinsic pathway, which is mediated by mitochondria [5, 10, 40]. The extrinsic pathway operates through the DRs, which are activated by binding their cognate ligands, such as TRAIL, a TNF-related apoptosis-inducing ligand that is a type II transmembrane protein [5, 13, 19, 45].

Four homologous human receptors for TRAIL have been identified. Two DRs, DR4/TRAIL-R1/TNFRSF10A and DR5/TRAIL-R2/TNFRSF10B [39, 41, 48], contain an extracellular cysteine-rich domain that recruits adaptor proteins, such as the Fas-associated death domain (FADD), and initiator CASPASES (PROCASPASES-8/10), thereby transducing the apoptotic signal [33, 34]. In contrast, neither the decoy receptor (TRAIL-R3/TRID/DcR1/

L. da Conceição Braga · L. M. Silva · J. B. Piedade
Serviço de Biologia Celular, Diretoria de Pesquisa e Desenvolvimento da Fundação Ezequiel Dias, Belo Horizonte, MG, Brazil

L. da Conceição Braga · P. Traiman · A. L. da Silva Filho
Departamento de Ginecologia e Obstetrícia da Faculdade de Medicina da, Universidade Estadual de São Paulo "Júlio de Mesquita Filho", Botucatu, SP, Brazil

A. L. da Silva Filho (✉)
Departamento de Ginecologia e Obstetrícia da Faculdade de Medicina da, Universidade Federal de Minas Gerais, Avenida Professor Alfredo Balena, 190, Santa Efigênia, Belo Horizonte, MG, Brazil
e-mail: agnaldo.ufmg@gmail.com

TNFRSF10C), which lacks a cytoplasmic domain [8, 39, 41], nor the TRAIL receptor 4 (TRAIL-R4/DcR2/TNFRSF10D), which contains a truncated cytoplasmic death domain, transduces apoptotic signals directly [7]. In this report, the TRAIL receptors are called TRAIL-R1, TRAIL-R2, TRAIL-R3 and TRAIL-R4.

The apoptotic signal transduced by TRAIL receptors can cause alterations in mitochondrial membrane integrity resulting in cytochrome c efflux and formation of the apoptosome [26]. In this context, *BCL2* (B-cell CLL/lymphoma 2) family members play a central role in regulating the intrinsic pathway. A total of 25 genes have been identified in the BCL2 family, which encode for a mix of proapoptotic and antiapoptotic proteins [16] that are classified by sequence homology in four α-helical segments from BH1 to BH4. The highly conserved antiapoptotic genes (e.g., *BCL2, BCL-X*, *BCL-XL*, *BCL-XS* and *BCL-WL*) contain all four BH domains, of which the BH1–BH3 domains structurally form a pocket capable of binding the BH3 domains of the other family proteins [45]. The antiapoptotic proteins BCL2 and BCL-XL bind and sequester the proapoptotic BH3-only proteins, thereby preventing BAX and BAK activation, or bind the activated conformers of BAX and BAK as a mechanism of cell survival [10]. A cell's susceptibility to apoptosis is influenced by the equilibrium of several components of both the proapoptotic and antiapoptotic proteins [1]. Because the TRAIL preference to kill tumor cells, it is a promising anti-cancer agent and the sensitivity to TRAIL-induced apoptosis is an important factor influencing the therapeutic response to TRAIL. However, the basis for the resistance and sensitivity of tumor cells to TRAIL-induced apoptosis is not completely understood [25]. TRAIL resistance could be mediated by a sort of defects in signaling pathway including inactivating mutations in *TRAIL-R1* and *TRAIL-R2*, loss of the initiator CASPASE-8 and BAX, and overexpression of BCL2 [36].

Furthermore, detachment from the extracellular matrix induces programmed cell death and this cell detachment-induced apoptosis has been a phenomenon called anoikis [25, 37, 44]. This special form of cell death is an important mechanism terminating the physiological cell life cycle by neglecting and is triggered by inadequate or inappropriate cell–matrix contacts [37] and it could be the second hypothesis to justify the resistance of tumor cells to TRAIL-induced apoptosis. Several authors postulate the involvement of the death receptors, like FADD and TRAIL protein, in anoikis with subsequent activation of CASPASE-8 led to cell death, generally through the intrinsic pathway that BCL2 family members play a central role in regulating [15]. BCL2 can interact with BMF (BCL-2-modifying factor) to act as sensitizer that binds pro-survival BCL-2 protein to displace activator proapoptotic BH3-only proteins (i.e., BID or BCL2-interacting mediator of cell death (BIM) [18]. After the cell has detached from the extracellular matrix, BIM and BMF are released from cytoskeleton, interact with protein BCL2 and neutralize its antiapoptotic action [18, 23]. Anoikis resistance may be explain in turn impacts metastatic aggressiveness by allowing cells to survive following detachment from the origin tissue matrix [23].

Epithelial ovarian cancer (EOC) is a silent disease that is usually diagnosed at an advanced stage and, currently, represents the most fatal gynecologic malignancy [2]. At the cellular and molecular levels, ovarian cancers are remarkably heterogeneous, a factor that makes EOC a difficult disease to treat effectively [2, 20, 27]. One of the major disappointments in the field of ovarian cancer research is the failure of the currently established therapies to cure tumors. More recent developments in apoptosis research have made it possible to devise novel therapeutic approaches that exploit this process to treat cancer. The observation that certain types of cancer express cell surface death receptors has triggered interest in exploring the potential of receptor ligation as a novel anti-cancer modality [32, 34]. However, for these agents to succeed, alone or in combination with other drugs, a deep understanding of their roles in specific signaling pathways and of how molecules in the tumor may interfere with the actions of these drugs is required. Otherwise, a promising strategy is to become ineffective due to the lack of tumor biology knowledge.

In this study, we aimed to investigate the expression of two apoptotic genes, *TRAIL-R2* and *BCL2*, to gain further insight into the apoptosis profile of EOC. Our postulate was that *TRAIL-R2* and *BCL2* expression in EOC could be considered to play an important role in resistance to apoptosis and/or anoikis which represents an unfavorable prognostic indicator for this type of human malignancy. Additionally, we investigated whether methylation at single CpGs regulates *TRAIL-R2* transcription. This strategy is used to identify the targets of epigenetic silencing in various tumor types, and DNA methylation is a frequent epigenetic event for the tumor suppressor genes that are active in many human cancers [29, 35, 43, 50].

Materials and methods

Patients and histology

Forty-five female patients were prospectively evaluated in the following three groups: serous EOC ($n = 16/45$), ovarian serous cystadenoma ($n = 11/45$) and normal ovary ($n = 18/45$). The study was performed in accordance with the Ethical Committee for Research in Human Beings

guidelines of the Institution. Informed consent was obtained from all patients involved in the study. Eligible cases were women with adnexal masses suggestive of malignancy who were scheduled to undergo cytoreductive surgery and pathologically confirmed diagnosis of serous epithelial ovarian cancer as soon as women with a uterine myoma who were scheduled to undergo total hysterectomy as clinically indicated. Tumor staging was performed according to the International Federation of Gynecology and Obstetrics (FIGO) recommendations [14]. The EOC patient samples were collected from the primary tumor ($n = 16/45$), and an additional sample of metastatic tumor was collected in the same patients when extra-pelvic disease larger than 1 cm was observed ($n = 5/16$). Normal ovarian epithelial tissue samples were taken from postmenopausal women who required a bilateral oophorectomy. After excision, the samples were immediately frozen in liquid nitrogen and stored at −80 °C for later use.

The isolation of RNA and genomic DNA (gDNA)

For RNA extraction, the preserved tissue samples (50–100 mg) were homogenized in 1 mL of TRIzol® (Life Technologies, Carlsbad, California, USA), and RNA from the tissues was isolated according to the manufacturer's instructions. The recovered RNA was then treated with an RNase-free DNase Set (Qiagen, Hilden, Germany). gDNA was isolated from the inter-organic phase of the TRIzol®-chloroform mixture and then combined with 0.7 mL of back extraction buffer (4 M guanidine isothiocyanate, 50 mM sodium citrate and 1 M Tris pH 8.0). After vigorous mixing by inversion, phase separation was achieved by centrifugation at 14,000×*g* for 15 min at 4 °C. The gDNA was then precipitated from the upper aqueous phase using 0.7 mL of isopropanol. The isolated gDNA from each fraction was dissolved in 20 μL of Milli-Q water and stored at −20 °C until use. The concentrations of the RNA or gDNA as well as the 260/280 absorbance ratio were measured using a NanoVuePathlength Calibration Fluid Kit (GE Healthcare, Little Chalfont, Buckinghamshire, UK).

cDNA synthesis

cDNA was generated from 2 mg of total RNA using Illustra Ready-to-Go RT-PCR Beads (GE Healthcare, Little Chalfont, Buckinghamshire, UK) in a total volume of 50 μL in accordance with the manufacturer's instructions.

Quantitative PCR analysis

The qRT-PCR was performed using an Agilent MX 3005P detection system (Stratagene, La Jolla, CA, USA). There were duplicate 10 μL reactions containing 1 X Brilliant II SYBR® Green QPCR Master Mix (Agilent Technologies, La Jolla, CA, USA); 0.2 μL of Rox (1:500); 0.25 μM of forward primer/0.20 μM of reverse primer for *TRAIL-R2* or *BCL2* and 0.2 μM of each primer for TATA binding protein (*TBP*), and 40 ng/μL cDNA (RNA equivalent) for each experiment.

The *TBP* was used as a reference locus for normalization. The sequences of the specific primers used in this study for *TBP* (GenBank ID: NM_003194) [30], *TRAIL-R2* (GenBank ID: NM_147187.2) [28] and *BCL2* (GenBank ID:666) (PrimerBank ID 6456033a2 [49]) have been previously reported.

The PCR cycling conditions were performed as follows: 95 °C for 10 min and 40 cycles of 95 °C for 30 s, annealing at 60 °C for 60 s and extension at 72 °C for 30 s.

The optimization of the qRT-PCR was performed according to the manufacturer's instructions. A sample without a template (no cDNA in the PCR) was included as a control in each assay. A melting curve was constructed for each primer pair to confirm product specificity. The 2[−Delta Delta C(T)] method was used to calculate the relative quantitation values from the data of an individual sample. The data for each sample were normalized with the normalizer gene for comparison with normal tissue, showing fold differences in *TRAIL-R2* and *BCL2* expression [31].

Bisulfite conversion

The gDNA was modified with sodium bisulfite using a Bisulfite Conversion Kit (Applied Biosystems, Foster City, USA) according to the manufacturer's instructions.

Methylation-specific polymerase chain reaction (MSP)

The MSP was performed as described previously [21]. *TRAIL-R2* Primer sets to amplify bisulfite-modified DNA were designed to produce a 102-base-pair PCR fragment. The primer sequences were unmethylated-specific 5′ TTATAGTTCGGGGCGTAGTC 3′ (sense) and 5′ AAATCT CGTCAACGCAATC 3′ (antisense) and methylated-specific 5′ AAATTATAGTTTGGGGTGTAGTT 3′ (sense) and 5′ AAAATCTCATCAACACAATCCT 3′ (antisense).

The MSP was performed in a total volume of 15 μL containing 10 ng of bisulfite-treated DNA, 1 X Epitech Master Mix (Qiagen, Hilden, Germany) and 0.3 μM of each primer. Reactions containing unmethylated DNA, methylated DNA or unmethylated bisulfite-converted DNA (Epitech Control DNA Set—Qiagen, Hilden, Germany) were performed as controls. The amplification was performed with the following conditions: 95 °C for 10 min; 35 cycles of 95 °C for 1 min, 60 °C for 1 min, and 72 °C

Table 1 Clinicopathological characteristics of the patients who provided the ovarian samples

	Normal ovary ($n = 18$)	Cystadenoma ($n = 11$)	EOC ($n = 16$)	p value
Age (years)	50.61 ± 2.13	54.3 ± 5.1	59.1 ± 2.7	0.128
Parity (births)	2.83 ± 0.44	2.3 ± 0.8	1.9 ± 0.3	0.356
CA-125 (U/mL)				
CA <330 (U/mL)		11 (100 %)	8 (50 %)	
CA >330 (U/mL)		0	8 (50 %)	
Tumor differentiation degree				
G2			6 (37.5 %)	
G3			10 (62.5 %)	
Cytoreduction				
Optimal (<1 cm)			7 (43.8 %)	
Suboptimal (>1 cm)			9 (56.3 %)	
Stage				
Stage I and II			5 (31.3 %)	
Stage III			8 (50 %)	
Stage IV			3 (18.7 %)	
Ascites				
Yes			10 (64.3 %)	
No			6 (35.7 %)	
Recurrence				
Yes			6 (37.5 %)	
No			10 (62.5 %)	
Mortality				
Yes			6 (37.5 %)	
No			10 (62.5 %)	
Menarche		12.8 ± 0.4	12.8 ± 3.4	0.991
Menopause				
Yes	18 (100 %)	6 (54.5 %)	13 (81.3 %)	0.008
No	0	5 (45.5 %)	3 (18.8 %)	

The values represent the mean ± standard error or n (percentage). The comparison between groups was performed using a χ^2 square test or an ANOVA as indicated. The median serum level of CA-125 was considered to determine the cut-off point. The tumor differentiation degree was classified as moderately differentiated (G2) or poorly differentiated (G3). Cytoreduction was considered optimal for a residual tumor <1 cm after tumor resection surgery. The tumor was staged according to the 2009 recommendations of FIGO (International Federation of Gynecology and Obstetrics). A p value ≤0.05 was considered to be statistically significant

EOC Epithelial ovarian carcinoma

for 30 s; and a final extension step for 10 min at 72 °C. The amplified MSP products (20 μL) were separated by electrophoresis onto 7.5 % non-denaturing polyacrylamide gels and visualized by silver nitrate staining.

Statistics

All statistical analyses were performed with the SPSS 18.0 software package (SPSS Inc., Chicago, IL, USA). The clinical data were expressed as a percentage and the mean ± standard error. The gene expression levels were expressed as the median with the interquartile range. The differences between the groups were evaluated using the χ^2, ANOVA, Mann–Whitney U and Kruskal–Wallis tests as indicated. A p value <0.05 was considered statistically significant.

Results

Patients

The patients included in this study were between 32 and 81 years old; the mean age was 54 ± 5 years ($p = 0.128$). The mean parity was 2.3 ± 0.3 births, with a range between 0 and 8 deliveries ($p = 0.356$). The only statistically significant difference between the groups was in the frequency of menopause ($p = 0.008$). The stage (FIGO)

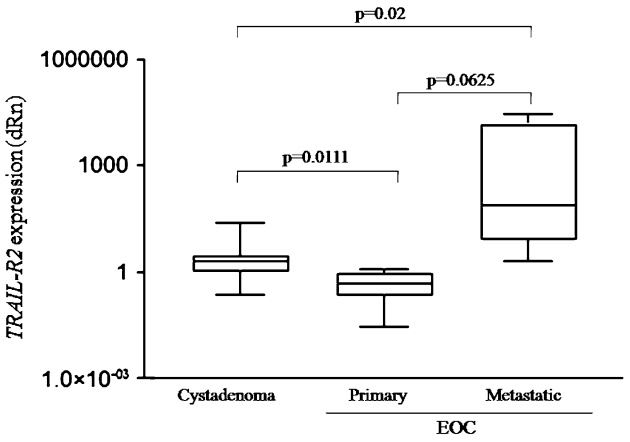

Fig. 1 The association of *TRAIL-R2* expression in ovarian tumors. The values shown represent the *TRAIL-R2* expression levels. The *horizontal line* indicates the median expression ratio, and the *box plots* demonstrate the interquartile range (25–75 %). The 10th–90th percentile ranges are also shown. The differences between groups were evaluated using a Mann–Whitney *U* test and Kruskal–Wallis test. *EOC* epithelial ovarian carcinoma

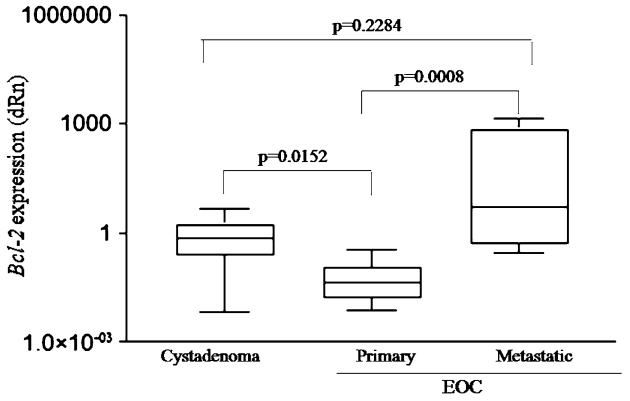

Fig. 2 The association of *BCL2* expression in ovarian tumors. The values shown represent the *BCL2* expression levels. The *horizontal line* indicates the median expression ratio, and the *box plots* demonstrate the interquartile range (25–75 %). The 10th–90th percentile ranges are also shown. The differences between groups were evaluated using a Mann–Whitney *U* test and Kruskal–Wallis test. *EOC* epithelial ovarian carcinoma

was I/II in 5 patients (31.3 %), III in 8 patients (50 %) and IV in 3 patients (18.7 %) in the EOC group.

The tumor was moderately differentiated (G2) in 6 (37.5 %) cases and poorly differentiated in 10 (62.5 %). The general sample characteristics are listed in Table 1.

The gene expression data

We identified *TRAIL-R2* and *BCL2* mRNA using qRT-PCR in all normal and ovarian tumor tissues, suggesting that the *TRAIL-R2* and *BCL2* genes are expressed in all cases (Figs. 1, 2).

The median *TRAIL-2* expression ratio in ovarian serous cystadenoma was 2.11 (1.04–2.71), and that in the primary EOC was 0.48 (0.21–0.09); the metastatic EOC expression ratio was 76.33 (7.66–14,502.47). Both the ovarian serous cystadenoma tumor and primary EOC groups had lower *TRAIL-R2* expression than the metastatic EOC samples (≥159.02-fold higher expression than the primary EOC group). Significant differences were observed in the *TRAIL-R2* expression levels when all the ovarian tumor groups were compared ($p = 0.0008$) as well as between the ovarian serous cystadenoma tumors and primary EOC and ovarian serous cystadenoma tumors and metastatic EOC group ($p = 0.01$ and $p = 0.02$, respectively). No statistical significance was observed when comparing primary EOC and metastatic EOC ($p = 0.06$) (Fig. 1).

For the *BCL2* expression levels, significant differences were observed when all the ovarian tumor groups were compared ($p = 0.03$). The median *BCL2* expression ratio in the ovarian serous cystadenoma was 0.8 (0.2–1.9), while in the primary EOC, the expression ratio was 0.4 (0.02–0.1). A significant difference in the *BCL2* expression level was observed between these groups ($p = 0.01$). In metastatic EOC, overexpression of *BCL2* was also detected with a median expression ratio of 5.4 (0.6–365.8). This level of *BCL2* expression was also significantly higher than the level found in primary EOC ($p = 0.0008$), although no statistical significance was seen when ovarian serous cystadenoma tumors were compared with metastatic EOC ($p = 0.2$) (Fig. 2).

The DNA methylation status of TRAIL-R2

With the use of primers specific for methylated or unmethylated *TRAIL-R2*, a product of 102 bp was detectable in both the positive controls from an MSP that used bisulfite-treated genomic DNA as the template. The results from the MSP products that were run onto 7.5 % non-denaturing polyacrylamide gels are shown in Fig. 3.

The methylation of at least one allele (hemimethylation) of *TRAIL-R2* was found in 40 % of the normal tissues, 40 % of the ovarian serous cystadenoma, 60 % of the primary EOC and 60 % of the metastatic EOC samples. However, no statistically significant associations were found between the methylation statuses of the *TRAIL-R2* promoter in these groups ($p = 0.87$) (Fig. 4).

Discussion

EOC is the deadliest gynecologic malignancy, and 80 % of patients who respond initially to treatment have recurrent disease and develop treatment resistance. Different latencies indicate the need for a better understanding of the

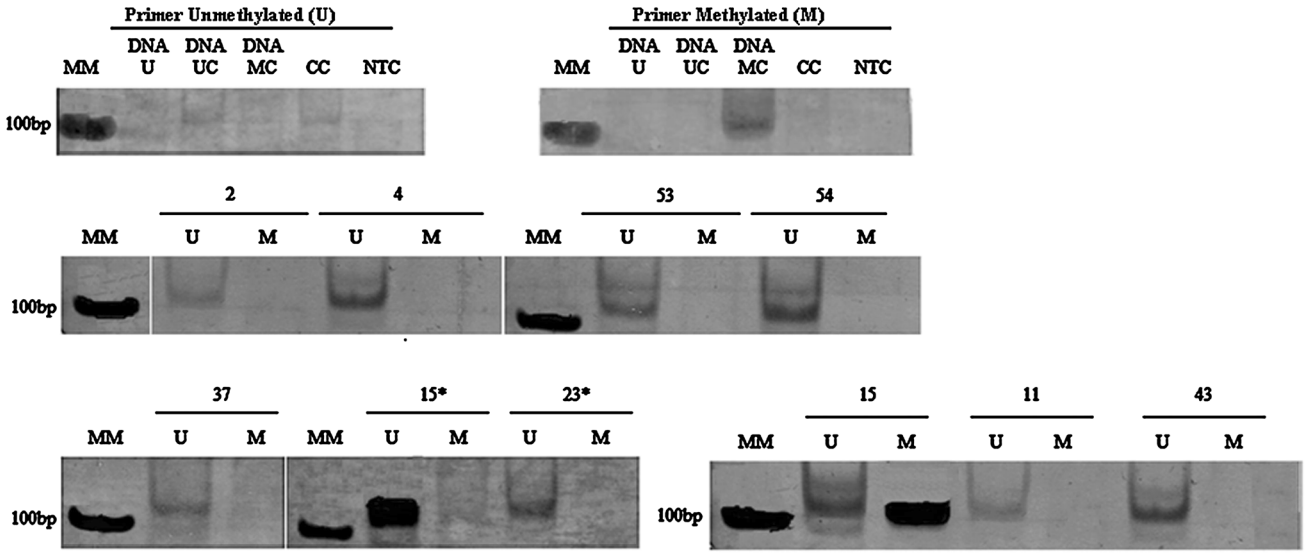

Fig. 3 An analysis of the CpG island promoter methylation status in *TRAIL-R2* by the methylation-specific polymerase chain reaction (MSP) assay. The 102-base-pair *TRAIL-R2* product was analyzed onto 7.5 % non-denaturing polyacrylamide gels. *U* represents the amplified products from primers specific to an unmethylated DNA sequence in the *TRAIL-R2* promoter, and *M* represents the amplified products from primers specific to a methylated sequence in the *TRAIL-R2* promoter. *MM* DNA molecular marker, *DNA U* unmethylated control DNA, *DNA UC* unmethylated control DNA after bisulfite conversion, *MC* bisulfite converted methylated control DNA (Qiagen, Hilden, Germany), which serves as a control for the methylated and unmethylated sequences; *CC* bisulfite converted control DNA that serves as a methylSEQr^{TM} bisulfite conversion control; case numbers 2 and 4: ovarian serous cystadenoma; 11, 15, 37 and 43: primary EOC; 15* and 23* metastatic EOC; 53 and 54 normal ovarian tissue. The sample was considered to be unmethylated when the product was detected with the primer U, and the sample was considered to be hemimethylated when the product was detected with the primers U and M

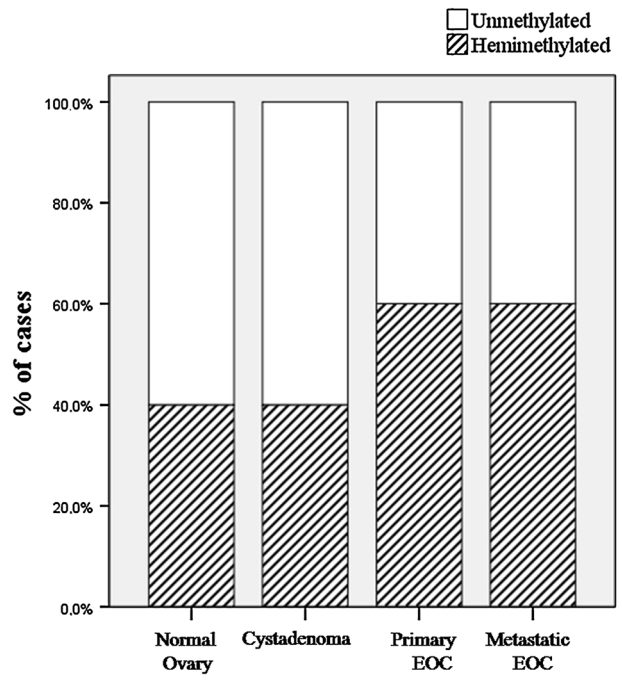

Fig. 4 The frequency of aberrant CpG island methylation in the *TRAIL-R2* promoter. Hemimethylation was detected in 40 % of the normal tissues, 40 % of the ovarian serous cystadenoma, 60 % of the primary EOC and 60 % of the metastatic EOC samples. No statistically significant associations between these groups were found by the Kruskal–Wallis test ($p = 0.87$)

disease and identification of new therapeutic targets or treatment modalities [2, 51].

Some factors have been identified in the study of drug resistance, such as the expression of multidrug resistance proteins, hypoxia in the tumor microenvironment, and resistance to apoptosis by the overexpression of survival factors and down-regulation of death signaling proteins [3]. In EOC, TRAIL signaling not only may influence the growth of cancer cells, but may also determine immunologic responses and could reflect the patient sensitivity or resistance to chemotherapy. Thus, it is the interplay of all of these factors that influences the disease endpoints and, ultimately, patient prognosis [12, 27, 40, 52]. To better understand the involvement of TRAIL-R2 and BCL2 on TRAIL signaling and apoptosis resistance in EOC, we evaluated the genetic expression and epigenetic variation of *TRAIL-R2* and the genetic expression of *BCL2* in ovarian serous cystadenoma, primary and metastatic EOC samples and normal ovarian tissues.

We demonstrated a higher *TRAIL-R2* expression level in metastatic EOC compared with ovarian serous cystadenoma and primary EOC. This result was calculated as a quantity relative to that in normal ovarian tissue, wherein the normal tissue sample was assigned an arbitrary quantity of "1" and all tumor samples were expressed in terms of their fold difference relative to the normal sample [31]. Our

results are consistent with the investigations of head and neck squamous cell carcinoma in which there was a significant down-regulation of *TRAIL-R2* expression in primary tumors [11].

Our study did not show any association between higher expression of *TRAIL-R2* observed in metastatic EOC and a survival advantage for patients. In agreement with our result, Elrod et al. [11] showed no survival advantage for metastatic head and neck squamous cell carcinoma that had high expression of *TRAIL-R2*. Indeed, in the cell lines from different cancers, including EOC, sensitivity to TRAIL was associated with high expression levels of the death receptors TRAIL-R1 and TRAIL-R2 and reduced expression levels of decoy receptors, such as TRAIL-R3 [27, 41]. These reports indicate that TRAIL signaling is more complex than originally anticipated and it can be accomplished in various ways, including a reduction of the death receptor, ligand, and effector protein levels or the up-regulation of antiapoptotic proteins [38].

Additionally, we examined the expression of *BCL2* family members that might contribute to a greater pro-survival effect and apoptosis resistance in EOC. We observed overexpression of *BCL2* in metastatic EOC, and this expression level was also significantly higher than in primary EOC. These results are consistent with those in the literature showing that BCL2 is overexpressed in several tumors (Burkitt's lymphoma, pancreatic carcinoma, melanoma, and neuroblastoma), and this increased expression is associated with increased proliferation and resistance to chemotherapy in many types of cancers, including EOC [6, 33]. Considering that antiapoptotic proteins can form heterodimers with multidomain proapoptotic proteins, such as BAX and BAK and that this interaction may prevent mitochondrial outer membrane permeabilization, which otherwise neutralizes the proapoptotic function [27]. The lower *BCL2* mRNA expression found in the primary EOC tissue samples could be made a biomarker favorable for the role of TRAIL in EOC, because it may increase apoptosis by TRAIL as well as ovarian cells can detach from their substrate and to involve in the subsequent cell death. In metastatic EOC, a relative resistance to death by apoptosis and the escape of tumors cells from anoikis could be explained by overexpression of *BCL-2* which inhibits apoptotic signal transduced by TRAIL-R2 and other BCL-2 family members that mediate anoikis.

The underexpression of *TRAIL*-R2 in primary EOC inspired us to analyze the mechanisms involved in its down-regulation. We looked for promoter hypermethylation, which can selectively down-regulate gene expression. In agreement with previous studies [42, 47], we found high frequencies of *TRAIL-R2* methylation in at least one allele of the gene in both normal and ovarian tumor tissues, but it is not in concordance with the loss of gene expression observed in ovarian serous cystadenoma and primary EOC. The *TRAIL-R2* hemimethylated alleles in metastatic EOC did not result in the gene expression silencing as observed in others human tumors [9, 22, 42]. There were no significant differences between the methylation profile and ovarian histological subtypes detected in our cohort, which was probably due to the limited number of patients and controls.

This study provides a useful basis for further analysis of epigenetic alterations in EOC and their controversial influence on gene expression, which is due to many reasons. First, the occasional reduction of *TRAIL-R2* expression that is observed with different DNA methylation levels could be explained by the lack of upstream transcription signals or by possible gene mutations [17, 24]. Second, the epigenetic silencing of gene transcription does not occur by promoter methylation changes alone but is mediated by a complex series of molecular events that cause remodeling of the chromatin configuration [17] as in some other tumors, such as small cell lung cancer [42]. Third, it is known that the methylation initiates at one or more chromosomal CpG sites in a promoter region and spreads to adjacent sites along the DNA strand until it meets a counteracting force in the form of open, active chromatin [17, 46]. Based on our previous findings of *TRAIL-R3* underexpression in primary EOC showing hemimethylation of the *TRAIL-R3* promoter frequently found in the neoplasia samples [4] and the fact that four receptors are mapped in a tandem fashion to the human chromosome 8p22-21, we can hypothesis that methylation (and resultant silencing) of the antiapoptotic *TRAIL-R3* genes may result in the silencing of the adjacent proapoptotic *TRAIL-R2* gene.

The absence of an association between the methylation data with the histological groups should be interpreted with caution. The most important limitation of this study is the relatively small number of patients and controls due to the low prevalence of the disease and ethical criteria control selected. Further studies with larger numbers of patients and longer follow-up are necessary to assess the accurate diagnostic and prognostic impact of *TRAIL-R2* and *BCL2* expression in EOC women.

In conclusion, the *TRAIL-R2* and *BCL2* genes exhibited differential expression between the tumor groups, and promoter DNA methylation appears an insufficient mechanism for *TRAIL-R2* gene silencing in primary EOC. We have highlighted the advantage of looking at two genes implicated in the same signaling pathway and the importance of a holistic approach when dealing with a specific pathway because the somatory effect of the deregulation of each member is what generates the downstream effects of the pathway. It remains to be determined in a larger series of patients whether these gene expressions can be used

clinically as markers of disease progression, either by themselves or in combination with other pathways.

Acknowledgments This work was supported by the Fundação de Amparo à Pesquisa do estado de Minas Gerais, FAPEMIG #PPM-CDS-00246-09, Coordenação de Aperfeiçoamento de Pessoal de Nível Superior, Capes and Conselho Nacional de Desenvolvimento Científico e Tecnológico, CNPq. The authors would like to thank Francisco de Oliveira Vieira for artwork help and the Pro-Rectory of Research of the Universidade Federal de Minas Gerais for additional financial support.

Conflict of interest The authors have no conflicts of interest to declare.

References

1. Bai M, Papoudou-Bai A, Horianopoulos N, Grepi C, Agnantis NJ, Kanavaros P (2007) Expression of bcl2 family proteins and active caspase 3 in classical Hodgkin's lymphomas. Hum Pathol 38:103–113
2. Bast RC Jr, Hennessy B, Mills GB (2009) The biology of ovarian cancer: new opportunities for translation. Nat Rev 9:415–428
3. Bevis KS, Buchsbaum DJ, Straughn JM Jr (2010) Overcoming TRAIL resistance in ovarian carcinoma. Gynecol Oncol 119:157–163
4. Braga L, Ramos A, Traiman P, Silva L, Silva-Filho A (2012) TRAIL-R3-related apoptosis: epigenetic and expression analyses in women with ovarian neoplasia. Gynecol Oncol 126:268–273
5. Bras M, Queenan B, Susin SA (2005) Programmed cell death via mitochondria: different modes of dying. Biochemistry 70:231–239
6. Debatin KM, Krammer PH (2004) Death receptors in chemotherapy and cancer. Oncogene 23:2950–2966
7. Degli-Esposti MA, Dougall WC, Smolak PJ, Waugh JY, Smith CA, Goodwin RG (1997) The novel receptor TRAIL-R4 induces NF-kappaB and protects against TRAIL-mediated apoptosis, yet retains an incomplete death domain. Immunity 7:813–820
8. Degli-Esposti MA, Smolak PJ, Walczak H, Waugh J, Huang CP, DuBose RF, Goodwin RG, Smith CA (1997) Cloning and characterization of TRAIL-R3, a novel member of the emerging TRAIL receptor family. J Exp Med 186:1165–1170
9. Elias A, Siegelin MD, Steinmuller A, von Deimling A, Lass U, Korn B, Mueller W (2009) Epigenetic silencing of death receptor 4 mediates tumor necrosis factor-related apoptosis-inducing ligand resistance in gliomas. Clin Cancer Res 15:5457–5465
10. Elmore S (2007) Apoptosis: a review of programmed cell death. Toxicol Pathol 35:495–516
11. Elrod HA, Fan S, Muller S, Chen GZ, Pan L, Tighiouart M, Shin DM, Khuri FR, Sun SY (2010) Analysis of death receptor 5 and caspase-8 expression in primary and metastatic head and neck squamous cell carcinoma and their prognostic impact. PLoS One 5:e12178
12. Falschlehner C, Emmerich CH, Gerlach B, Walczak H (2007) TRAIL signalling: decisions between life and death. Int J Biochem Cell Biol 39:1462–1475
13. Fariss MW, Chan CB, Patel M, Van Houten B, Orrenius S (2005) Role of mitochondria in toxic oxidative stress. Mol Interv 5:94–111
14. FIGO IFoGaO (2009) Clinical practice guidelines
15. Frankel A, Rosen K, Filmus J, Kerbel RS (2001) Induction of anoikis and suppression of human ovarian tumor growth in vivo by down-regulation of Bcl-X(L). Cancer Res 61:4837–4841
16. Fulda S, Debatin KM (2006) Extrinsic versus intrinsic apoptosis pathways in anticancer chemotherapy. Oncogene 25:4798–4811
17. Gronbaek KHC, Jones PA (2007) Epigenetic changes in cancer. APMIS 115:10
18. Hausmann M, Leucht K, Ploner C, Kiessling S, Villunger A, Becker H, Hofmann C, Falk W, Krebs M, Kellermeier S, Fried M, Scholmerich J, Obermeier F, Rogler G (2011) BCL-2 modifying factor (BMF) is a central regulator of anoikis in human intestinal epithelial cells. J Biol Chem 286:26533–26540
19. Hengartner MO (2000) The biochemistry of apoptosis. Nature 407:770–776
20. Hennessy BT, Murph M, Nanjundan M, Carey M, Auersperg N, Almeida J, Coombes KR, Liu J, Lu Y, Gray JW, Mills GB (2008) Ovarian cancer: linking genomics to new target discovery and molecular markers: the way ahead. Adv Exp Med Biol 617:23–40
21. Herman JG, Graff JR, Myohanen S, Nelkin BD, Baylin SB (1996) Methylation-specific PCR: a novel PCR assay for methylation status of CpG islands. Proc Natl Acad Sci USA 93:9821–9826
22. Hopkins-Donaldson S, Ziegler A, Kurtz S, Bigosch C, Kandioler D, Ludwig C, Zangemeister-Wittke U, Stahel R (2003) Silencing of death receptor and caspase-8 expression in small cell lung carcinoma cell lines and tumors by DNA methylation. Cell Death Differ 10:356–364
23. Igney FH, Krammer PH (2002) Death and anti-death: tumour resistance to apoptosis. Nat Rev Cancer 2:277–288
24. Imura M, Yamashita S, Cai LY, Furuta J, Wakabayashi M, Yasugi T, Ushijima T (2006) Methylation and expression analysis of 15 genes and three normally-methylated genes in 13 ovarian cancer cell lines. Cancer Lett 241:213–220
25. Jin Z, McDonald ER 3rd, Dicker DT, El-Deiry WS (2004) Deficient tumor necrosis factor-related apoptosis-inducing ligand (TRAIL) death receptor transport to the cell surface in human colon cancer cells selected for resistance to TRAIL-induced apoptosis. J Biol Chem 279:35829–35839
26. Kelly MM, Hoel BD, Voelkel-Johnson C (2002) Doxorubicin pretreatment sensitizes prostate cancer cell lines to TRAIL induced apoptosis which correlates with the loss of c-FLIP expression. Cancer Biol Ther 1:520–527
27. Khaider NG, Lane D, Matte I, Rancourt C, Piche A (2012) Targeted ovarian cancer treatment: the TRAILs of resistance. Am J Cancer Res 2:75–92
28. Kim K, Fisher MJ, Xu SQ, el-Deiry WS (2000) Molecular determinants of response to TRAIL in killing of normal and cancer cells. Clin Cancer Res 6:335–346
29. Lai JCWJ, Cheng YW, Yeh KT, Wu TC, Chen CY et al (2009) O6-methylguanine-DNA methyltransferase hypermethylation modulated by 17beta-estradiol in lung cancer cells. Anticancer Res 29:6
30. Li YYF, Hua Y, Lu W, Xie X (2009) Identification of suitable reference genes for gene expression studies of human serous ovarian cancer by real-time polymerase chain reaction. Anal Biochem 394:7
31. Livak KJ, Schmittgen TD (2001) Analysis of relative gene expression data using real-time quantitative PCR and the 2[−Delta Delta C(T)] method. Methods 25:402–408
32. Mahmood Z, Shukla Y (2010) Death receptors: targets for cancer therapy. Exp Cell Res 316:887–899
33. Malhi H, Gores GJ (2006) TRAIL resistance results in cancer progression: a TRAIL to perdition? Oncogene 25:7333–7335
34. Mellier G, Huang S, Shenoy K, Pervaiz S (2010) TRAILing death in cancer. Mol Asp Med 31:93–112
35. Meng CFZX, Peng G, Dai DQ (2009) Promoter histone H3 lysine 9 di-methylation is associated with DNA methylation and aberrant expression of p16 in gastric cancer cells. Oncol Rep 22:7

36. Min KJ, Jang JH, Lee JT, Choi KS, Kwon TK (2012) Glucocorticoid receptor antagonist sensitizes TRAIL-induced apoptosis in renal carcinoma cells through up-regulation of DR5 and down-regulation of c-FLIP(L) and Bcl-2. J Mol Med (Berl) 90:309–319
37. Nagaprashantha LD, Vatsyayan R, Lelsani PC, Awasthi S, Singhal SS (2011) The sensors and regulators of cell-matrix surveillance in anoikis resistance of tumors. Int J Cancer 128: 743–752
38. Ouellet V, Le Page C, Madore J, Guyot MC, Barres V, Lussier C, Tonin PN, Provencher DM, Mes-Masson AM (2007) An apoptotic molecular network identified by microarray: on the TRAIL to new insights in epithelial ovarian cancer. Cancer 110:297–308
39. Pan G, Ni J, Wei YF, Yu G, Gentz R, Dixit VM (1997) An antagonist decoy receptor and a death domain-containing receptor for TRAIL. Science 277:815–818
40. Pavet V, Portal MM, Moulin JC, Herbrecht R, Gronemeyer H (2011) Towards novel paradigms for cancer therapy. Oncogene 30:1–20
41. Sheridan JP, Marsters SA, Pitti RM, Gurney A, Skubatch M, Baldwin D, Ramakrishnan L, Gray CL, Baker K, Wood WI, Goddard AD, Godowski P, Ashkenazi A (1997) Control of TRAIL-induced apoptosis by a family of signaling and decoy receptors. Science 277:818–821
42. Shivapurkar N, Toyooka S, Toyooka KO, Reddy J, Miyajima K, Suzuki M, Shigematsu H, Takahashi T, Parikh G, Pass HI, Chaudhary PM, Gazdar AF (2004) Aberrant methylation of trail decoy receptor genes is frequent in multiple tumor types. Int J Cancer 109:786–792
43. Suzuki HGE, Chen W, Anbazhagan R, Van Engeland M, Weijenberg MP et al (2002) A genomic screen for genes upregulated by demethylation and histone deacetylase inhibition in human colorectal cancer. Nat Genet 31:9
44. Taddei ML, Giannoni E, Fiaschi T, Chiarugi P (2012) Anoikis: an emerging hallmark in health and diseases. J Pathol 226:380–393
45. Taylor RC, Cullen SP, Martin SJ (2008) Apoptosis: controlled demolition at the cellular level. Nat Rev 9:231–241
46. Turker MS (2002) Gene silencing in mammalian cells and the spread of DNA methylation. Oncogene 21:5388–5393
47. van Noesel MM, van Bezouw S, Salomons GS, Voute PA, Pieters R, Baylin SB, Herman JG, Versteeg R (2002) Tumor-specific down-regulation of the tumor necrosis factor-related apoptosis-inducing ligand decoy receptors DcR1 and DcR2 is associated with dense promoter hypermethylation. Cancer Res 62: 2157–2161
48. Walczak H, Degli-Esposti MA, Johnson RS, Smolak PJ, Waugh JY, Boiani N, Timour MS, Gerhart MJ, Schooley KA, Smith CA, Goodwin RG, Rauch CT (1997) TRAIL-R2: a novel apoptosis-mediating receptor for TRAIL. EMBO J 16:5386–5397
49. Wang X, Seed B (2003) A PCR primer bank for quantitative gene expression analysis. Nucleic Acids Res 31:e154
50. Wu Y, Alvarez M, Slamon DJ, Koeffler P, Vadgama JV (2010) Caspase 8 and maspin are downregulated in breast cancer cells due to CpG site promoter methylation. BMC Cancer. doi:10.1186/1471-2407-10-32
51. Yap TA, Carden CP, Kaye SB (2009) Beyond chemotherapy: targeted therapies in ovarian cancer. Nat Rev 9:167–181
52. Yerbes R, Palacios C, Lopez-Rivas A (2011) The therapeutic potential of TRAIL receptor signalling in cancer cells. Clin Transl Oncol 13:839–847

Advances in Brief

Molecular Determinants of Response to TRAIL in Killing of Normal and Cancer Cells[1]

Kunhong Kim, Michael J. Fisher, Shi-Qiong Xu, and Wafik S. El-Deiry[2]

Laboratory of Molecular Oncology and Cell Cycle Regulation, Howard Hughes Medical Institute, Departments of Medicine, Pharmacology, Genetics, Cancer Center, and the Institute for Human Gene Therapy, University of Pennsylvania School of Medicine, Philadelphia, Pennsylvania 19104

Abstract

The tumor necrosis factor-related apoptosis-inducing ligand (TRAIL or Apo2L) is a potent inducer of death of cancer but not normal cells, which suggests its potential use as a tumor-specific antineoplastic agent. TRAIL binds to the proapoptotic death receptors DR4 and the p53-regulated proapoptotic KILLER/DR5 as well as to the decoy receptors TRID and TRUNDD. In the present studies, we identified a subgroup of TRAIL-resistant cancer cell lines characterized by low or absent basal DR4 or high expression of the caspase activation inhibitor FLIP. Four of five TRAIL-sensitive cell lines expressed high levels of DR4 mRNA and protein, whereas six of six TRAIL-resistant cell lines expressed low or undetectable levels of DR4 (χ^2; $P < 0.01$). FLIP expression appeared elevated in five of six (83%) TRAIL-resistant cell lines and only one of five (20%) TRAIL-sensitive cells (χ^2; $P < 0.05$). Two TRAIL-resistant lines that expressed DR4 contained an A-to-G alteration in the death domain encoding arginine instead of lysine at codon 441. The K441R polymorphism is present in 20% of the normal population and can inhibit DR4-mediated cell killing in a dominant-negative fashion. The expression level of KILLER/DR5, TRID, TRUNDD or TRID, and TRUNDD did not correlate with TRAIL sensitivity ($P > 0.05$). These results suggest that the major determinants for TRAIL sensitivity may be the expression level of DR4 and FLIP. TRAIL-resistant cells became susceptible to TRAIL-mediated apoptosis in the presence of doxorubicin. In TRAIL-sensitive cells, caspases 8, 9, and 3 were activated after TRAIL treatment, but in TRAIL-resistant cells, they were activated only by the combination of TRAIL and doxorubicin. Our results suggest: (*a*) evaluation of tumor DR4 and FLIP expression and host DR4 codon 441 status could be potentially useful predictors of TRAIL sensitivity, and (*b*) doxorubicin, in combination with TRAIL, may effectively promote caspase activation in TRAIL-resistant tumors.

Introduction

TRAIL[3], a member of the TNF cytokine family and a type II membrane protein, was initially identified by homology to the C-terminal extracellular domain of other TNF family members, such as Fas ligand (FasL), TNF-α, and lymphotoxin α (1). TRAIL is a potent inducer of apoptosis in a variety of transformed or cancer cells of human and mouse origin but not normal cells (1, 2).

The therapeutic use of the Fas/FasL or the TNF-α/TNFR1 system in cancer treatment has been hampered by severe side effects (3). The systemic administration of TNF causes a septic shock-like response possibly mediated by nuclear factor-κB activation, and the injection of agonist Ab to Fas can be lethal (3, 4). Compared to TNF-α or Fas, TRAIL may be a safer alternative because normal cells appear to be resistant, and it activates nuclear factor-κB only weakly (5). Recently, evidence for the safety and potential efficacy of TRAIL therapy against breast and colon cancer was obtained in a severe combined immunodeficiency mouse model (6, 7). Additionally, in cell culture, the human leucine zipper (LZ)-TRAIL had no cytotoxic effects on normal cells, including human mammary epithelial cells, human renal proximal tubule epithelial cells, human lung fibroblasts, and human skeletal muscle cells but was toxic toward mammary adenocarcinoma cells (6). The *in vivo* experiments showed that the systemic administration of LZ-TRAIL into mice inoculated with breast cancer cells prolonged survival. These studies suggest that TRAIL may have a potential use for cancer treatment.

TRAIL can modulate an apoptotic response by binding to one of four cell-surface receptors: Death receptor (DR) 4 (TRAIL-R1; Ref. 8), KILLER/DR5 (TRAIL-R2, TRICK2; Refs. 9–12), TRID (DcR1, TRAIL-R3, or LIT; Refs. 5, 10, 13, and 14), and TRUNDD (DcR2 or TRAIL-R4; Refs. 15–17). DR4 and KILLER/DR5 have two cysteine-rich extracellular ligand-binding domains and a cytoplasmic death domain that signals downstream caspase activation (2, 18). KILLER/DR5 was identified as a candidate p53 target gene, linking DNA

Received 12/15/98; revised 10/29/99; accepted 10/29/99.
The costs of publication of this article were defrayed in part by the payment of page charges. This article must therefore be hereby marked *advertisement* in accordance with 18 U.S.C. Section 1734 solely to indicate this fact.
[1] Supported in part by NIH Grants CA75138-01 and CA75454-01.
[2] To whom requests for reprints should be addressed, at the Laboratory of Molecular Oncology and Cell Cycle Regulation, Howard Hughes Medical Institute, University of Pennsylvania School of Medicine, 415 Curie Boulevard, CRB 437A, Philadelphia, PA 19104. Fax: (215) 573-9139.

[3] The abbreviations used are: TRAIL, tumor necrosis factor-related apoptosis-inducing ligand; Ab, antibody; TNF, tumor necrosis factor; MTT, 3-(4,5-dimethylthiazol-2-yl)-2,5-diphenyltetrazolium bromide; GAPDH, glyceraldehyde-3-phosphate dehydrogenase; RT-PCR, reverse transcription-PCR; TRUNDD, TRAIL decoy receptor containing a truncated death domain; TRID, TRAIL decoy receptor lacking an intracellular domain; KILLER/DR5, p53-regulated proapoptotic KILLER/death receptor 5; FLIP, FLICE inhibitory protein; PARP, poly ADP-ribose polymerase; FADD, FAS-associated death domain protein; CMV-β-gal, cytomegalovirus β-galactosidase; mAb, monoclonal Ab.

damage signaling from p53 to downstream caspase activation and cell death (9). The extracellular domain of TRID shares a homology with DR4 and KILLER/DR5, but it does not have a cytoplasmic death domain, and it is anchored to the membrane through a glycosyl phosphatidyl inositol linkage. TRUNDD has a substantially truncated cytoplasmic death domain. These two decoy receptors have been reported to protect cells from TRAIL-mediated apoptosis by competing with DR4 and KILLER/DR5 for binding to TRAIL (10).

The TRAIL-mediated biochemical signaling pathway leading to apoptosis is not yet clear. Previously, it was reported that the ectopic expression of FADD-DN (dominant-negative FADD, which blocks apoptotic signaling by the Fas/APO1 death receptor) does not efficiently block apoptosis triggered by TRAIL, and that overexpression of DR4 could induce apoptosis in FADD-deficient embryonic fibroblasts (19). These studies suggest that a FADD-independent pathway may link TRAIL to the caspase cascade (2, 19, 20). Moreover, it was shown that DR4 does not efficiently recruit FADD, TNF receptor-associated death domain (TRADD) protein, receptor interacting protein (RIP), or RIP-associated ICH-1/CED-3 homologous protein (RAIDD; Ref. 10). Although at present there is a missing link between TRAIL death receptors and caspase activation, it is clear that once TRAIL binds to its receptors, apoptosis ensues through the activation of caspases (5, 8, 10). Initiator caspases (caspases 8, 9, and 10) are composed of an N-terminal prodomain that contains the region for homotypic protein-protein interaction with adaptor molecules together with one large and one small subunit. When cells receive death-inducing signals, the prodomain is cleaved, and an active heterodimeric tetramer containing two small and two large subunits is formed. It was reported that caspases 3 and 8 became activated when HeLa cells were treated with TRAIL (21) and also that in TRAIL-sensitive breast cancer cell lines, caspase 3 cleavage was observed (22). In addition, a recent report that T lymphocytes that have catalytically inactive caspase 10 are TRAIL-resistant implicates caspase 10 in TRAIL-mediated apoptosis (23).

Although the efficacy and potential use of TRAIL in cancer treatment has been suggested, little is known about the factors that determine the sensitivity of cancer cells to killing by TRAIL. Recently, there were some reports on the determinants of TRAIL sensitivity in breast cancer cells (22), melanoma (24), and brain tumors (25, 26). The results have been somewhat controversial in that some reports showed no correlation between TRAIL sensitivity and the expression level of proapoptotic death receptors, whereas others demonstrated a correlation between them.

We investigated the expression level of various TRAIL receptor family members as determinants for TRAIL sensitivity and whether a DNA-damaging chemotherapeutic drug such as doxorubicin might have additive effects with TRAIL in killing cancer cells. We report here that the expression of the proapoptotic TRAIL receptors, in particular DR4, and the caspase activation inhibitor FLIP may be major determinants of TRAIL sensitivity. In addition to the expression level of DR4, a polymorphism found in the death domain region of DR4 prevents DR4-mediated cell killing in a dominant-negative fashion. Finally, we also report that a DNA damaging agent such as doxorubicin can sensitize cells to TRAIL-mediated cell killing. Our results provide essential preclinical information that may be useful in the design of clinical trials using recombinant TRAIL in the therapy of human cancer.

Materials and Methods

Cell Lines. Human lung fibroblast WI38 and human foreskin fibroblast HS27 cells were obtained from the American Type Culture Collection (Rockville, MD). The human ovarian cancer cell line SKOV3, the human breast cancer cell line SKBr3, and the human nasopharyngeal squamous cancer cell line FADU were also obtained from the American Type Culture Collection. The human lung cancer cell lines H460 Neo/E6, the human colon cancer cell lines HCT116 Neo/E6, the human ovarian cancer cell lines PA1 Neo/E6, and the human colon cancer cell line SW480 were maintained as described previously (27). The J82 human bladder cancer cell line was a gift from T. McGarvey and B. Malkowicz (University of Pennsylvania, Philadelphia, PA), and the A875 human melanoma cell line was a gift from D. George (University of Pennsylvania, Philadelphia, PA).

Assessment of Cell Viability. Recombinant soluble human TRAIL was purchased from Kamiya Biomedical Co. (Seattle, WA), and the anti-FLAG M2 mAb was purchased from Sigma (Saint Louis, MI). Three thousand cells were seeded into each well of a 96-well plate. After 24 h, the cells were treated with TRAIL (200 ng/ml) and cross-linked with the anti-FLAG M2 mAb (2 μg/ml). Cell viability was measured by using the MTT assay at 16 h after treatment (28). When normal cells were treated with both doxorubicin and TRAIL, the cells were treated with increasing concentrations of chemotherapeutic drugs alone (doxorubicin, 0, 0.1, 1, 10, and 100 μg/ml) or in combination with TRAIL (20 ng/ml) cross-linked with the anti-FLAG M2 Ab (2 μg/ml). To assess the long-term effect of TRAIL, a total of 5×10^4 of each cell line were seeded in triplicate into 24 wells, and at 24 h, cells were treated with TRAIL (50 ng/ml) and the anti-FLAG M2 Ab (2 μg/ml). The media containing TRAIL and Ab was changed every 48 h, and the culture was maintained for 7 days, at which time the remaining cells were stained with Coomassie Blue.

Semiquantitative RT-PCR. Total RNA was isolated from cell lines as described (29). cDNA was generated from 2 μg of total RNA in a final volume of 20 μl using SuperScript II (Life Technologies, Inc., Gaithersburg, MD) and random primers. The sequences of specific primers used in this experiment were as follows: DR4 F, 5′-CGATGTGGTCAGAGCTGGTACAGC-3′; DR4 R, 5′-GGACACGGCAGAGCCTGTGCCATC-3′; KILLER/DR5 F, 5′-GGGAGCCGCTCATGAGGAAGTTG G-3′, KILLER/DR5 R, 5′-GGCAAGTCTCTCTCCCAGCGTCTC-3′; TRID F, 5′-GTTTGTTTGAAAGACTTCACTGTG-3′, TRID R, 5′-GCAGGCGTTTCTGTCTGTGGGAAC-3′; TRUNDD F, 5′-CTTCAGGAAACCAGAGCTTCCCTC-3′, TRUNDD R, 5′-TTCTCCCGTTTGCTTATCACACGA-3′; GAPDH F, 5′-ACCACAGTCCATGCCATCAC-3′, GAPDH R, 5′-TCCACCACCCTGTTGCTGTA-3′.

To analyze the expression level of the death receptors, 2 μl (out of 20 μl) of synthesized cDNA was amplified in a total volume of 50 μl containing 200 μM each of all four dNTPs, 2 μCi α-^{32}P-dCTP (3000 Ci/mmol), 2 μM each of death receptor-

specific primer set along with 2 μM each of the GAPDH primers, and 1 unit of *Taq* DNA polymerase (Perkin-Elmer). The cycle numbers that showed linear growth of product were initially determined for each PCR product by analyzing a 10-μl sample from multiple identical amplification reactions (Fig. 2*A* and data not shown). In the case of DR4 and KILLER/DR5, 23 cycles were chosen; for TRID and TRUNDD, 24 cycles were chosen; and in the case of GAPDH, 18 cycles were chosen. During PCR, 10 μl of the reaction were remove at the indicated cycle numbers. PCR conditions were as follows: 1 cycle, 5 min/95°C; 23 or 24 cycles, 30 s/95°C, 30 s/55°C (for DR4, KILLER/DR5, and TRUNDD), 52°C (for TRID), or 30 s/72°C. Nondenaturing PAGE (7%) was performed, and the gel was fixed, dried, and autoradiographed. Band intensities were quantitated by using a Phosphorimager Storm 840 (Molecular Dynamics, Sunnyvale, CA).

Genomic DNA Isolation and Cycle Sequencing. Whole blood (20 ml) from 10 normal healthy volunteers was drawn, and genomic DNA was isolated using the Blood and Cell culture DNA maxi kit (QIAGEN Inc., Valencia, CA). The DNA (50 ng) was used as a template for the amplification of the DR4 death domain region spanning nucleotide 1322. Sequences of primers used in PCR are as follows: DR4 11, 5′-CTCTGATGCTGTTCTTTGAC-3′, DR4 12, 5′-TCACTCCAAGGACACGGCAGA-3′. After amplification, each PCR product was visualized and purified from an agarose gel using the QIAquick gel extraction kit (QIAGEN Inc.) and was then used as a DNA sequencing template. Cycle sequencing was performed using a SequiTherm cycle sequencing kit (Epicentre Technologies, Madison, WI) according to the manufacturer's instructions.

Site-directed Mutagenesis and Sequencing. Site-directed mutagenesis was performed using a Quick change site-directed mutagenesis kit (Stratagene, La Jolla, CA) according to the manufacturer's instructions. To change a base in the death domain region of DR4 (A to G at nucleotide 1322 of DR4), plasmids that contained either the full-length DR4 (f/DR4 (A) in pCEP4, Invitrogen, Carlsbad, CA) or the cytoplasmic domain of DR4 (CD/DR4 (A) in pcDNA3.1-Myc, His; Invitrogen, Carlsbad, CA) were used as templates. The sequences of the primer pairs used for changing the base were as follows: DR4DDMUT F,5′-GGAAGAGAGACATGCAA*G*AGAGAAGATTCAGGACC-3′; DR4DD MUT R, 5′-GGTCCTGAATCTTCTCT*C*TTGCATGTCTCTCTTCC-3′. The sequences of the mutagenized plasmids were confirmed. Sequencing of expression plasmids was performed using a T7 DNA sequencing kit (United States Biochemicals, Cleveland, OH) according to the manufacturer's instructions.

The mutagenized f/DR4 or CD/DR4 was used for transfection into SW480 colon cancer cells as previously described (30). After 24 h of transfection, cell lysates were prepared from each transfectant followed by Western immunostaining for confirmation of expression after mutagenesis.

Evaluation of Cell Death Induced by Transfected DR4. For cell death evaluation, cotransfection of the CMV-β-gal marker gene and the DR4 mutant constructs generated was performed as previously described (31). Briefly, 1×10^5 of SW480 cells were plated per well in 24-well plates and transfected with 2 μg of the corresponding parental vectors, f/DR4 (A), CD/DR4 (A), f/DR4 (G), or CD/DR4 (G), with CMV-β-gal at 10% of the total amount of DNA. At 24 or 48 h later, cells were fixed and stained with 5-bromo-4-chloro-3-indolyl-β-galactopyranoside to quantify the number of blue cells. To determine whether polymorphic DR4 has a dominant-negative effect on cell killing, SW480 cells were transfected with variable ratios of CD/DR4 (A) to CD/DR4 (G), f/DR4 (A) to CD/DR4 (G), or f/DR4 (A) to f/DR4 (G) (4:1, 1:1, and 1:4) along with CMV-β-gal.

Abs and Western Blot Analysis. Western blot analysis was carried out as previously described (32). Blotted membranes were immunostained with anti-PARP (1:2000; Boehringer Mannheim, Mannheim, Germany), anti-caspase 3 (E-8, 1:500; Santa Cruz Biotechnologies, Inc., Santa Cruz, CA), anti-caspase 7 (1:500; PharMingen, San Diego, CA), anti-caspase 8 (C-20, 1:500; Santa Cruz Biotechnologies, Inc.), anti-caspase 9 (1:500; IIMGENEX, San Diego, CA), anti-caspase 10 (N-19, 1:500; Santa Cruz Biotechnologies, Inc.), anti-caspase 2 (H-19, 1:500; Santa Cruz Biotechnologies, Inc.), anti-DR4 (1:500, PharMingen), anti-DR5 (1:500; IMGENEX,) anti-FLIP (1:500; IMGENEX), anti-Myc (9E10, 1:500; Santa Cruz Biotechnologies, Inc.), or antiactin (I-19, 1:200; Santa Cruz Biotechnologies, Inc.).

Statistical Analysis. The statistical correlation between the expression level of TRAIL death receptors and TRAIL-mediated apoptosis was performed using regression analysis and the correlation between the expression of FLIP and TRAIL sensitivity, or the expression of DR4 and TRAIL sensitivity was performed using the χ^2 test.

Results

Normal Cells as Well as a Newly-defined Subset of Cancer Cells Are Resistant to TRAIL-mediated Apoptosis. We evaluated the cell killing effect of TRAIL on various normal and cancer cell lines. As previously reported by others (1, 3), normal cells (fibroblasts) were resistant to TRAIL treatment (Fig. 1, *A* and *B*). In contrast, cancer cells showed a variable response to TRAIL (Fig. 1). HCT116, H460, PA1, SKBr3, and SW480 were sensitive to TRAIL. TRAIL sensitivity was defined as a <75% cell viability at 16 h after TRAIL treatment is measured by the TRAIL MTT assay. A875, FADU, J82, and SKOV3 cells were found to be resistant to TRAIL. Human Papillomavirus E6-expressing HCT116, H460, and PA1 cells were relatively more resistant to TRAIL than the neocounterparts (Fig. 1*A*). Long-term (7 days) TRAIL treatment of cell lines (Fig. 1*B*) showed nearly the same result as the short-term (16 h) MTT assay results. Based on the observations from the long-term TRAIL treatment assay, certain fractions of cells showed resistance to TRAIL, although the majority of the cells were killed by TRAIL treatment.

Taken together, those results suggest that there is a subgroup of TRAIL-resistant cancer cells and that to a degree, wild-type p53 may modulate TRAIL responsiveness. We further explored the molecular basis of TRAIL resistance in cancer cells.

Correlation between TRAIL Receptor Expression and TRAIL Sensitivity. To determine whether there is any correlation between TRAIL sensitivity and the expression level of TRAIL receptors, a semiquantitative RT-PCR assay was per-

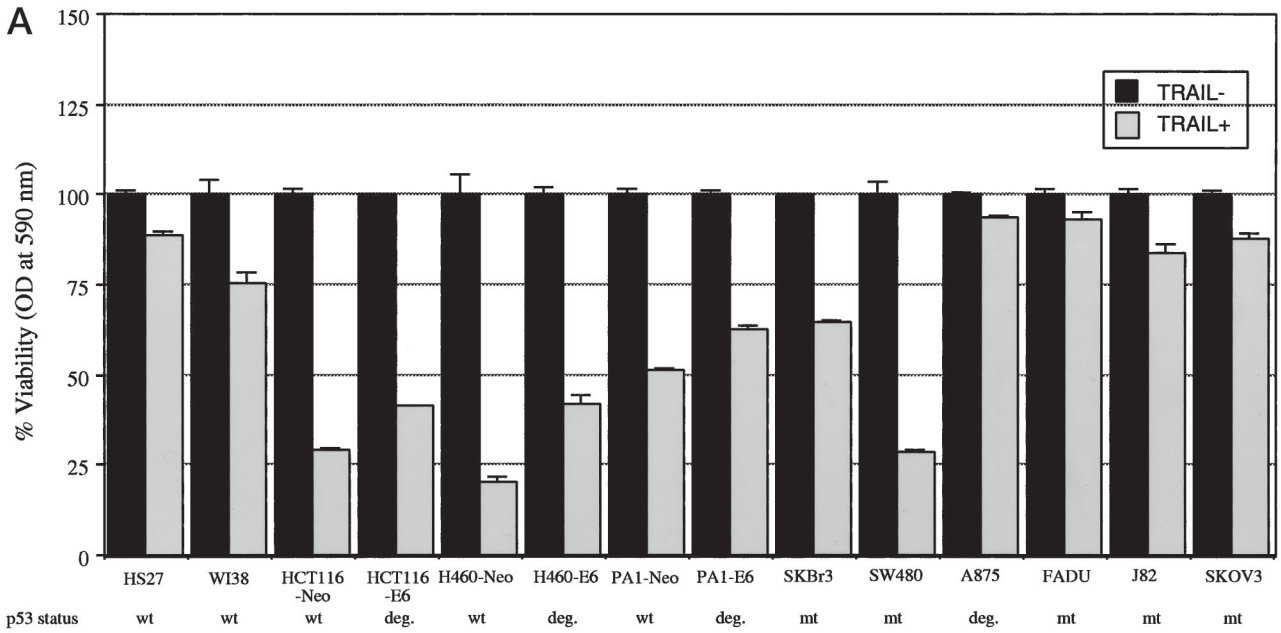

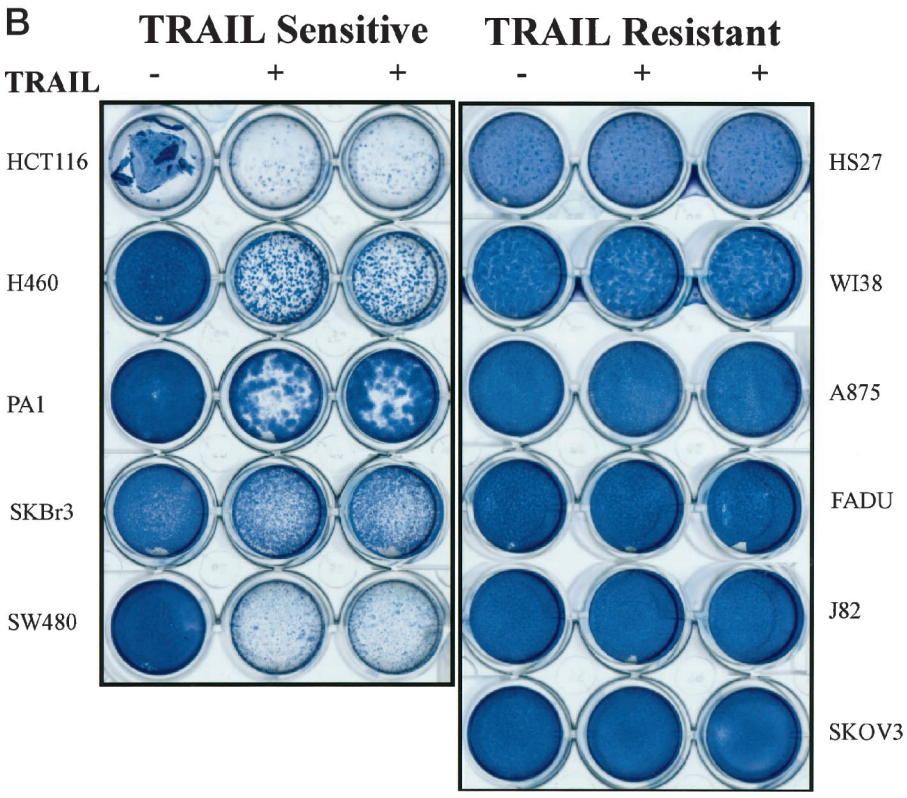

Fig. 1 *A*, transient and long-term assays reveal variable cytotoxic effects of TRAIL toward normal and cancer cells. Cell viability was evaluated by the MTT assay (See "Materials and Methods"). Cells were incubated for 16 h in the absence (*black bar*) or presence (*gray bar*) of TRAIL (200 ng/ml) and the anti-FLAG M2 mAb (2 μg/ml). The status of the p53 tumor suppressor gene is indicated below the bars for each cell line. *wt*, wild type; *mt*, mutant; *deg*, degraded by HPV E6 or MDM2 (in the case of the A875 cell line that overexpresses MDM2; Ref. 32). All samples were tested in quadruplicate (value ± SD). *B*, long-term (7 days) assays of the TRAIL effect on cell killing. A total of 5×10^4 cells were seeded in triplicate into each well of a 24-well plate. Cells were either treated with TRAIL (50 ng/ml) and the anti-FLAG M2 Ab (*TRAIL*+) or treated with only Ab (*TRAIL*−). After 7 days of treatment, cells were stained with Coomassie Blue.

formed (Fig. 2). The number of PCR cycles required for linear amplification and detection was initially determined for each death receptor (Fig. 2*A*). KILLER/DR5 was expressed in all cell lines tested (Fig. 2, *B* and *C*), and its mRNA expression level did not correlate with TRAIL sensitivity (Fig. 3*B*). In contrast, the expression level of DR4 varied among different cell lines (Fig. 2*B*). For example, in normal fibroblast cells, DR4 expression was very low or not detectable (Fig. 2*B*, *Lanes 1* and *2*). Cancer cell lines except J82 and SKOV3 that expressed DR4 were sensitive to TRAIL regardless of p53 status (Fig. 1, Fig. 2*B*, and Fig. 3*A*; see below). PA1, A875, and FADU cells did not express detectable DR4 protein (Fig. 2*B*, *Lanes 5*, *6*, and *9*). DR4 protein was highly expressed in HCT116, H460, and SW480 cells (DR4 in Fig. 4, *Lanes 3*, *4*, and *7*), and they were the most sensitive cell lines to TRAIL (Fig. 1, *A* and *B*). The antiapoptotic TRAIL receptors, TRID and TRUNDD, were also

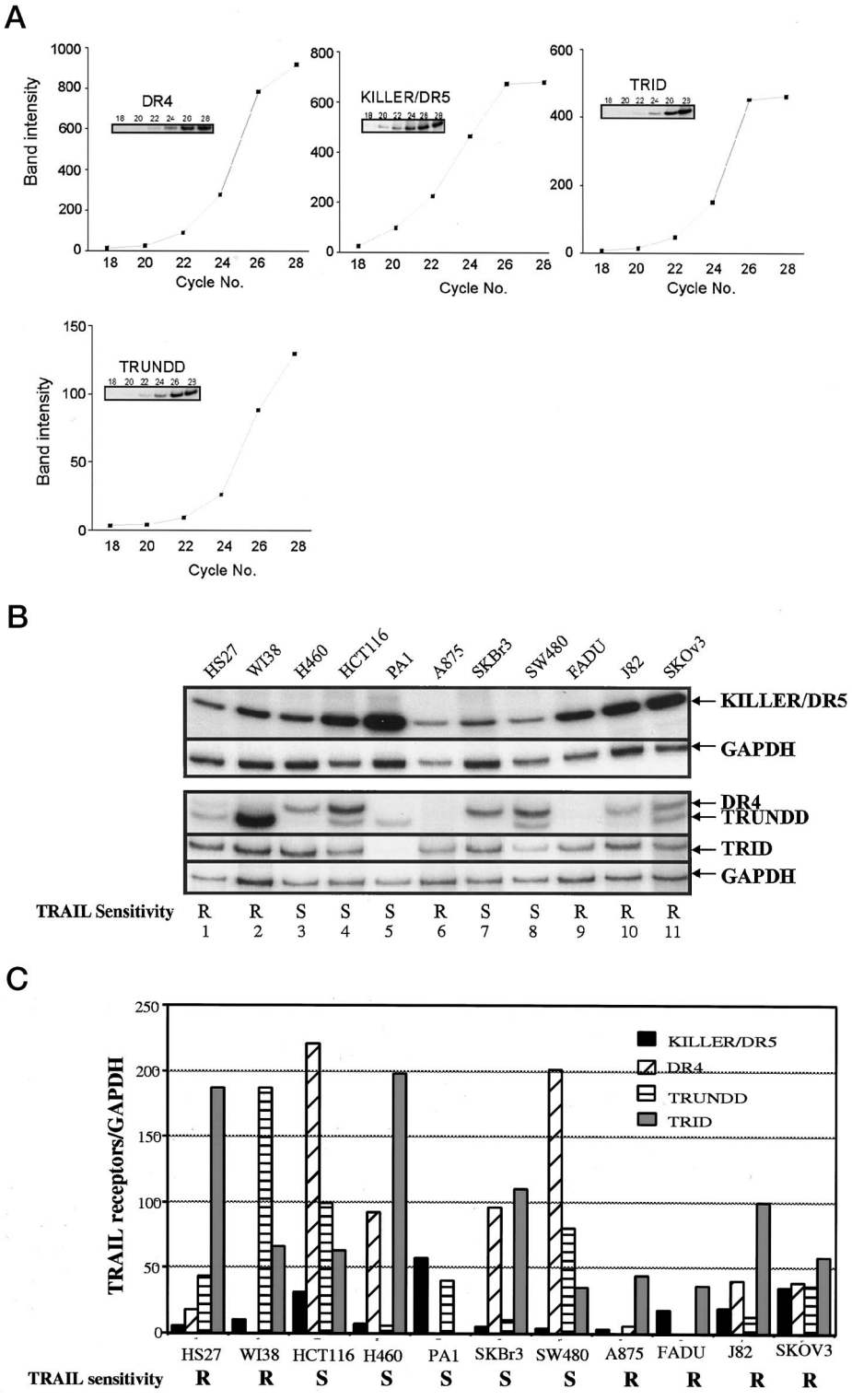

Fig. 2 Expression level of TRAIL death receptor genes in normal and cancer cells. *A*, kinetics of amplification of mRNA using a semiquantitative-labeled RT-PCR assay (see "Materials and Methods"). Autoradiograms are shown in the *inset* for each experiment, with PCR cycle numbers shown above different lanes. *B*, expression of TRAIL receptor genes using the semiquantitative RT-PCR assays as described in the text. *C*, relative expression of TRAIL receptors normalized with GAPDH expression.

expressed in cancer cells. TRID was expressed in all of the cell lines except PA1 cells, whereas TRUNDD was not expressed in H460, A875, SKBr3, and FADU cell lines (Fig. 2*B, Lanes 3, 6, 7*, and *9*). The high expression of TRID or TRUNDD in the normal cell lines HS27 or WI38 is consistent with previous results implicating high decoy receptor expression as a mechanism of TRAIL resistance. However, neither TRID nor TRUNDD levels adequately explain the observed patterns of

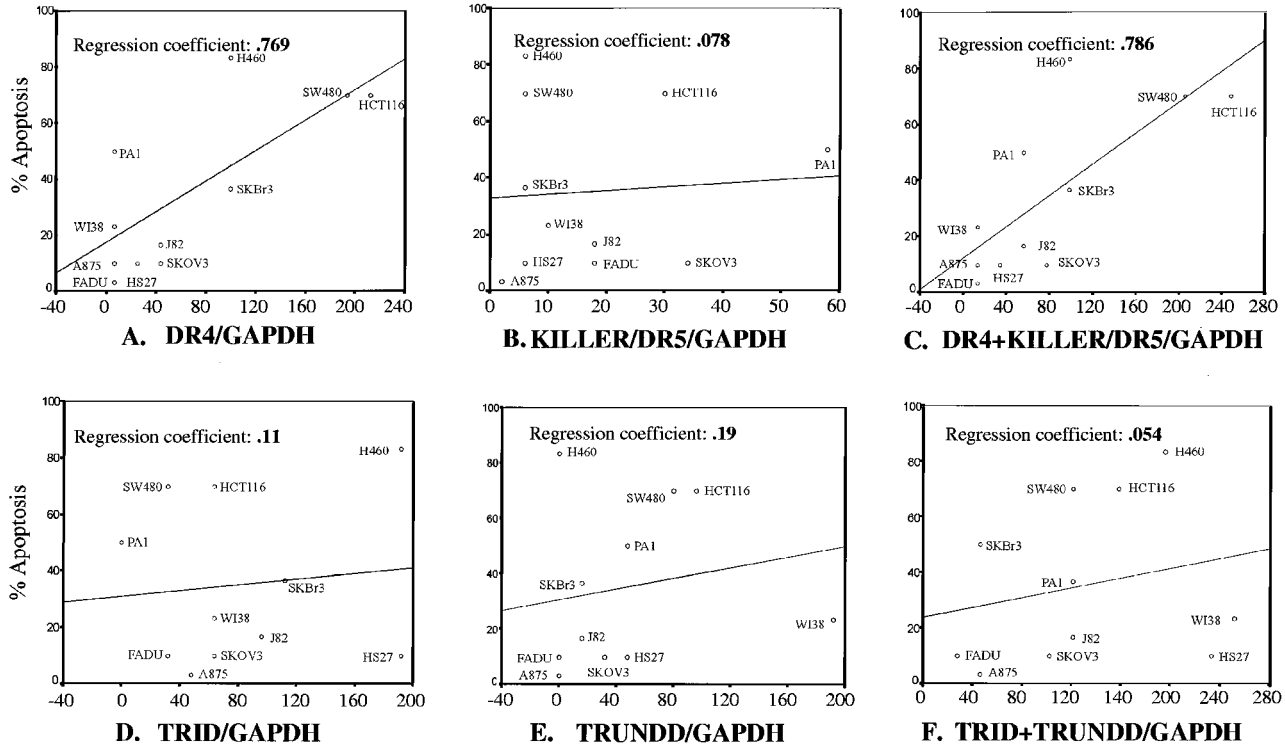

Fig. 3 Regression analysis of the relation between TRAIL-mediated apoptosis and the expression level of death receptors normalized to GAPDH expression. *A*, *B*, *D*, and *E*, the result obtained from regression analysis between TRAIL-mediated apoptosis *versus* the expression level (determined by RT-PCR) of each TRAIL death receptor. *C* and *F*, the result obtained from regression analysis between TRAIL-mediated apoptosis *versus* the sum of the expression level of the proapoptotic TRAIL death receptors and the antiapoptotic TRAIL death receptors. The regression coefficient for the relation between apoptosis and expression of DR4 or DR4+KILLER/DR5 was 0.769 and 0.786, respectively ($P = 0.006$ and 0.004, respectively).

TRAIL sensitivity in the panel of cancer cells (Fig. 3, *D-F*). The presence of DR4 alone ($r = 0.769$; $P = 0.006$) or DR4 and KILLER/DR5 ($r = 0.786$, $P = 0.004$) appeared to correlate better with TRAIL sensitivity of cancer cells than the expression of decoy receptors (Fig. 3, *A* and *C*).

FLIP Expression Correlates Well with TRAIL Resistance. Cellular FLIP is an inhibitor of caspase activation and may be overexpressed in human cancer cells (33). We determined whether the expression level of FLIP might correlate with TRAIL sensitivity. We detected FLIP expression in five of six TRAIL-resistant cell lines including normal cells A875, J82, and SKOV3 (FLIP in Fig. 4, *Lanes 1, 2, 8, 10,* and *11*) but only in one (PA1) of five TRAIL-sensitive cell lines (FLIP in Fig. 4, *Lane 5*). These results suggest that high expression of FLIP may be the another important determinant of TRAIL resistance (χ^2; $P < 0.05$).

K441R Polymorphism Found in the Death Domain of DR4. Contrary to our expectation that DR4-expressing cells should be sensitive to TRAIL, J82 and SKOV3 were resistant to TRAIL treatment. Previously, there was a report indicating that Fas carrying a mutation in the death domain region could act as a dominant-negative inhibitor of Fas-induced cell killing (25). To investigate whether there is a DNA sequence change in the death domain of DR4 in J82 and SKOV3 cells, RT-PCR and DNA sequencing was performed. Sequencing results showed that there is an A-to-G alteration in nucleotide 1322 of DR4 both in SKOV3 and J82 cells (Fig. 5*A* and data not shown). This A-to-G transition resulted in the conversion of the amino acid lysine (codon 441) to arginine. To determine whether this alteration is present in normal populations, genomic DNA was isolated from total blood drawn from 10 normal healthy volunteers, and PCR cycle sequencing was performed. The results revealed that 2 (donor 1 and 10) of 10 (20%) normal individuals have the base change (Fig. 5*B*), and thus, we refer to the alteration as a polymorphism. The polymorphism was found in donors 1 and 10, and SKOV3 was heterozygous in all cases (Fig. 5*B*).

Effect of the K441R Polymorphism in the Death Domain of DR4 on DR4-mediated Cell Killing. To determine whether the K441R polymorphism has any effect on DR4-mediated cell killing, we generated DR4 mammalian expression constructs containing the polymorphism by using site-directed mutagenesis (Fig. 6, *A* and *B*). Upon transfection, we found that polymorphic DR4 was less effective in cell killing than its wild-type counterpart (Fig. 6, *C* and *D*). In addition, polymorphic DR4 showed an inhibitory effect toward cell killing by wild-type DR4. A potent dominant-negative effect of the K441R polymorphism was observed when the cytoplasmic DR4 (CD/DR4) was expressed. The CD/DR4 (G) rather than f/DR4 (G) showed a nearly complete inhibition of DR4-mediated cell killing (Fig. 6*D*).

These results suggest, at least in terms of TRAIL sensitiv-

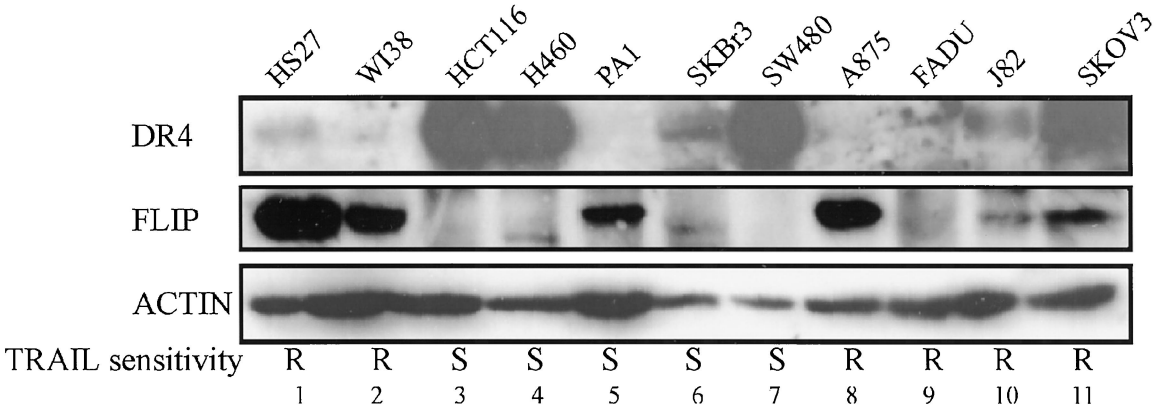

Fig. 4 Protein expression of DR4 and FLIP. Cell lysates were prepared from each cell line, and an equal amount of protein was loaded on a 15% SDS-PAGE gel. Western immunoblotting was performed with anti-DR4 and anti-FLIP Ab. Actin was used as an internal control for protein loading.

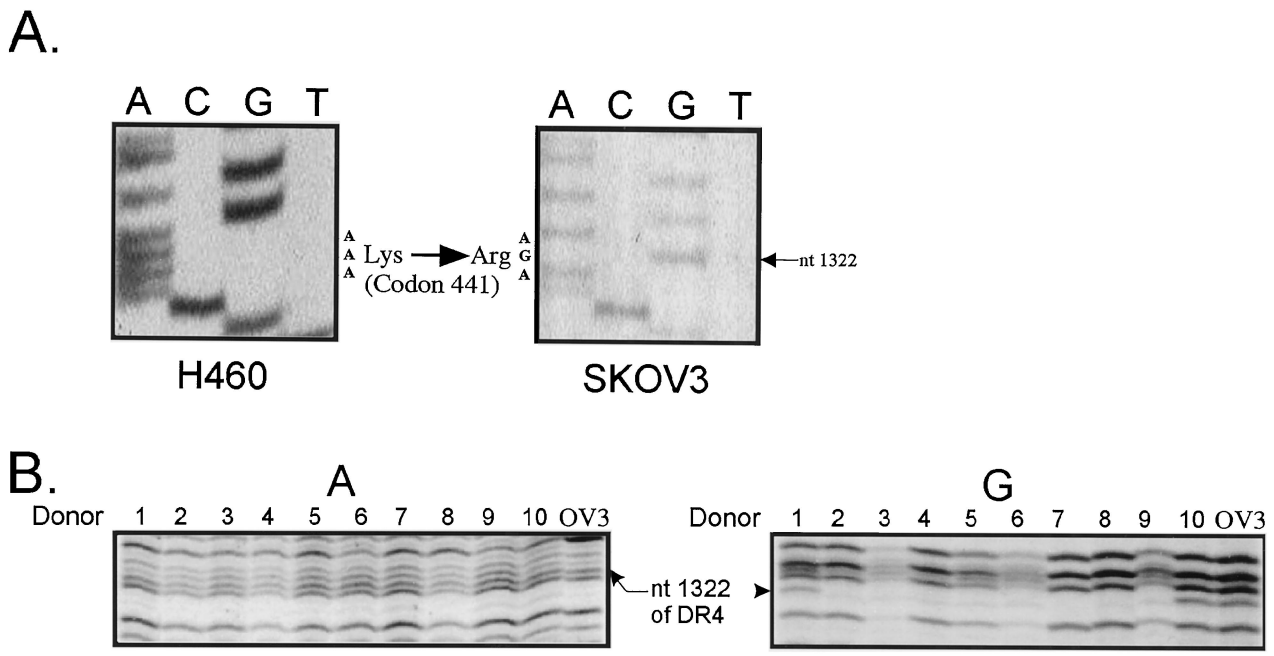

Fig. 5 K441R polymorphism found in the death domain of DR4. *A,* A-to-G transition at nucleotide 1322 of DR4 in SKOV3 cells. RT-PCR was performed as described in the text. PCR products were cloned into a TA cloning vector (Invitrogen) followed by sequencing using cloned plasmid as a template. Approximately 50% of the clones contained the K441R polymorphism. TRAIL-sensitive DR4-expressing cell lines such as H460 (and HCT116, data not shown) have A at nucleotide 1322, but resistant cell lines such as SKOV3 (and J82, data not shown) have G encoding arginine instead of lysine at codon 441. *B,* A-to-G transition is found in a normal population. PCR amplification using genomic DNA isolated from whole blood of normal healthy donors as a template was performed and followed by cycle sequencing. Samples from each termination mix were loaded together for easy comparison. Donors 1 and 10 showed A-to-G transition, and also, they were heterozygous. SKOV3 also shows an A-to-G transition and is heterozygous.

ity, that the K441R polymorphism in the death domain of DR4 makes cells relatively resistant to TRAIL treatment, although they express DR4 on their cell surface. Thus, this polymorphism found in J82 and SKOV3 could contribute to TRAIL resistance.

Cell Killing by Combination of Doxorubicin and TRAIL in TRAIL-resistant Cell Lines. Normal cells such as HS27 and WI38 are resistant to TRAIL in part due to a low or undetectable expression of DR4, a high expression level of decoy receptors, and a high expression level of FLIP (Fig. 2 and Fig. 4). However, when these cells were treated with the combination of doxorubicin and TRAIL, viability was dramatically reduced (Fig. 7*A*) and PARP cleavage became evident (Fig. 7*B*). Western immunostaining (Fig. 7*C*) showed that there was a significant induction of KILLER/DR5 protein expression. This

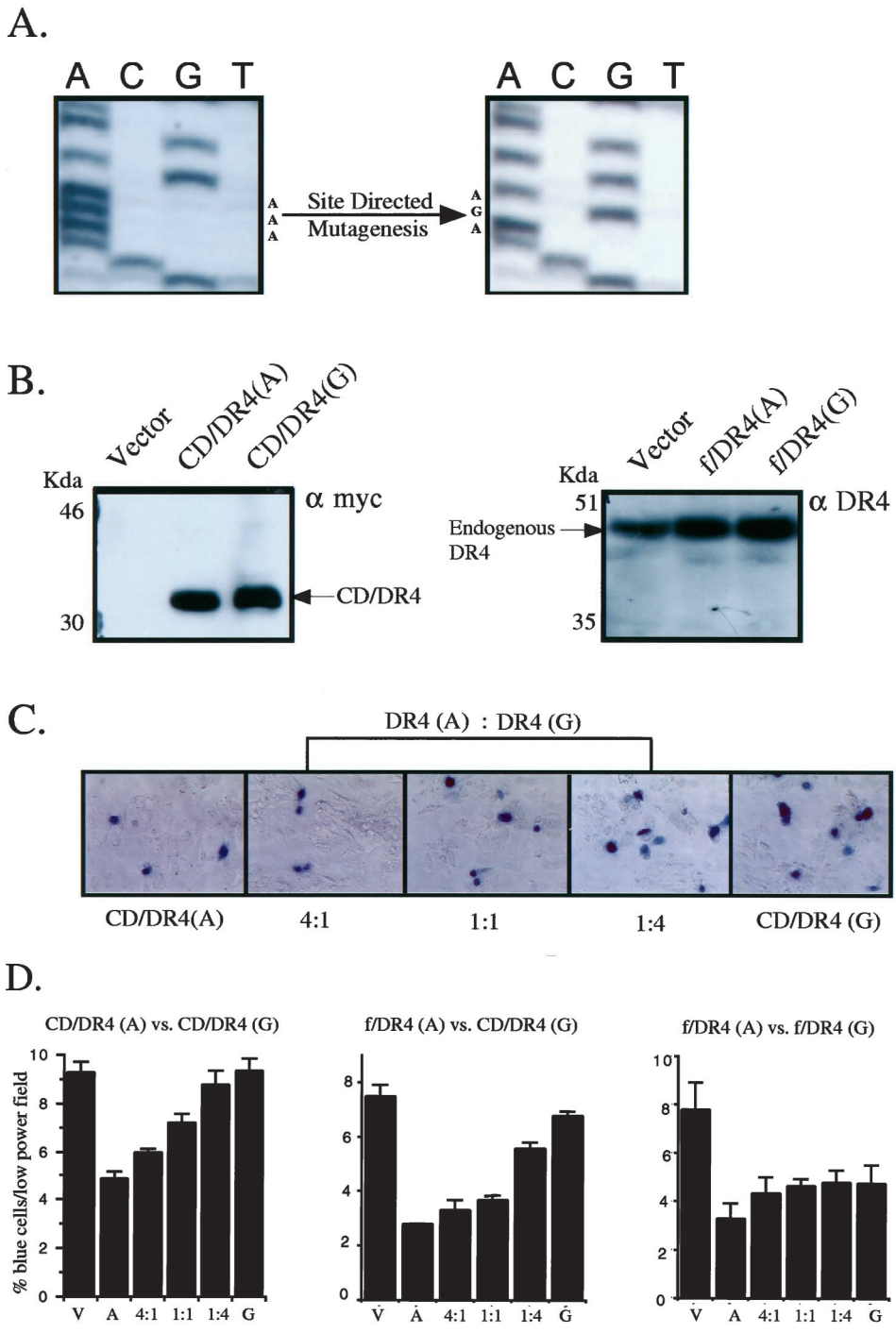

Fig. 6 Functional effect of the polymorphism on the DR4-mediated cell killing. *A*, site-directed mutagenesis of a DR4 expression plasmid. F/DR4 (A) or CD/DR4 (A) that can express a full-length or cytoplasmic domain of DR4 cloned in pCEP4 or pcDNA 3.1, respectively, was used for mutagenesis. Mutagenesis was confirmed by sequencing. The resulting constructs were named f/DR4 (G) or CD/DR4 (G). *B*, Western blot analysis to confirm the protein expression of CD/DR4 and f/DR4 constructs before and after mutagenesis. SW480 cells were transfected with each DR4 expressing construct. At 20 h after transfection, cell lysates were prepared, and Western immunoblotting was performed using anti-DR4 for f/DR 4 or anti-Myc for CD/DR4. *Arrow*, myc-tagged CD/DR4. *C*, SW480 cells were cotransfected with variable ratios of CD/DR4 (A) to CD/DR4 (G), as indicated, and CMV-β-gal (at 10% of the total DNA) for 48 h. Cells were then stained for the β-galactosidase activity with 5-bromo-4-chloro-3-indolyl-β-D-galactopyranoside. The same high power fields (×320) are shown under phase-contrast microscopy. *D*, dominant-negative effect of polymorphic DR4 on wild-type DR4. The number of blue cells per low power field (×100) was quantified after transfection of SW480 cells as described in *C*. All samples were tested in quadruplicates (value ± SD). *V*, vector; *A*, wild-type DR4; *G*, polymorphic DR4.

induction of KILLER/DR5 by doxorubicin may sensitize normal cells to TRAIL-mediated cell killing. These results suggest that an increase in the ratio of expression between proapoptotic and antiapoptotic molecules may reset the responsiveness of the cells from resistant to sensitive. There was no change in the level of DR4 or FLIP expression after doxorubicin treatment (Fig. 7*C*).

p53 function was compromised in all of the TRAIL-resistant cancer cell lines tested in this study either by mutation (J82, FADU, and SKOV3) or by the overexpression of MDM2 (A875; Ref. 32). Thus, an exposure to a DNA damaging agent such as doxorubicin might not be expected to result in the p53-dependent KILLER/DR5 induction observed in the normal cells. Nevertheless, when those cells were treated with both

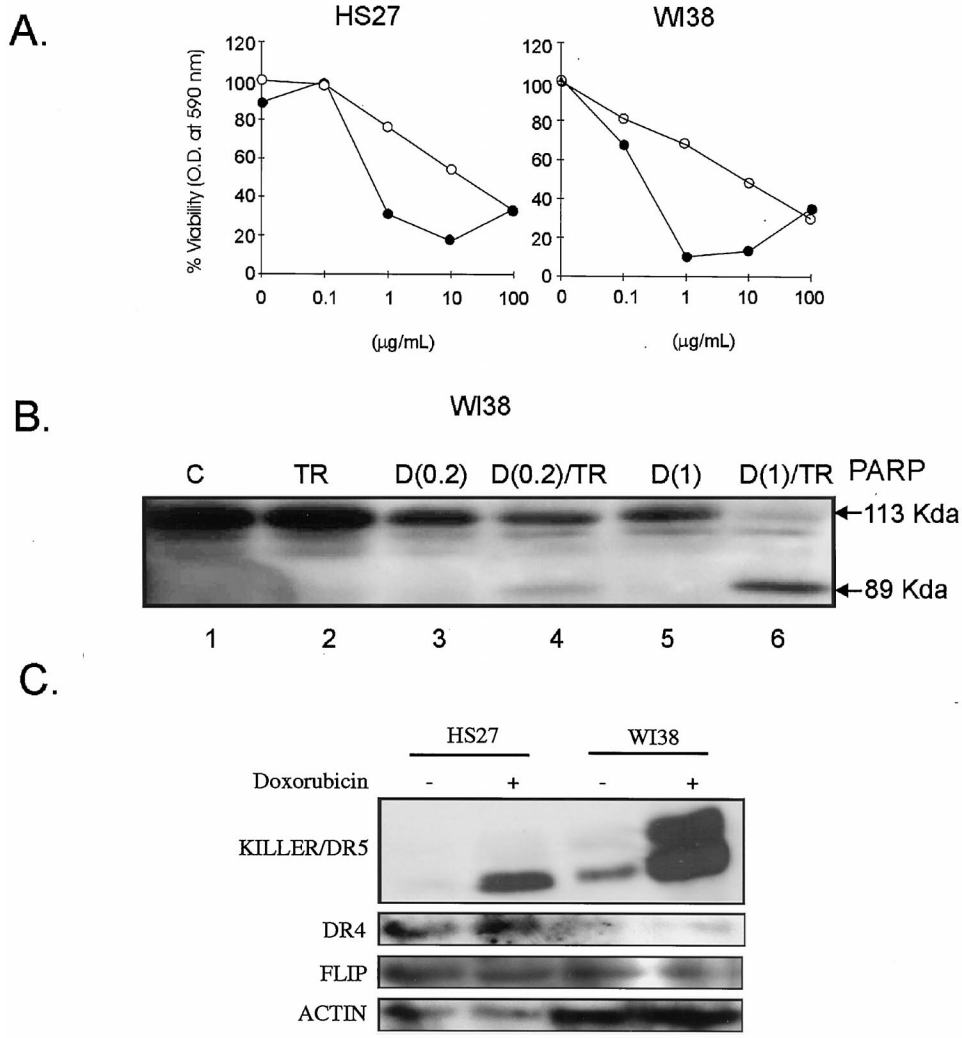

Fig. 7 KILLER/DR5 but not DR4 induction after doxorubicin exposure correlates with an enhanced sensitivity of normal cells to TRAIL-mediated apoptosis. *A,* effect of combined treatment of doxorubicin and TRAIL on viability of HS27 or WI38. Cells were treated with varying concentrations of doxorubicin in the absence (*open circles*) or presence (*solid circles*) of TRAIL (20 ng/ml) and anti-FLAG M2 mAb (2 μg/ml) for 16 h. Cell viability was evaluated by MTT assay. *B,* cleavage of PARP occurs upon treatment of WI38 with TRAIL and doxorubicin. *C* represents control cells (*Lane 1*); *TR* represents cells treated with TRAIL only (*Lane 2*); *D(0.2)* represents cells treated with doxorubicin (0.2 μg/ml; *Lane 3*); *D(0.2)/TR* represents cells treated with doxorubicin (0.2 μg/ml) and TRAIL (*Lane 4*); *D(1)* represents cells treated with doxorubicin (1 μg/ml; *Lane 5*); and *D(1)/TR* represents cells treated with doxorubicin (1 μg/ml) and TRAIL (*Lane 6*). *C,* Western blot analysis revealed that there was an induction of KILLER/DR5 but no change in DR4 or FLIP expression after doxorubicin treatment. Actin was used as an internal control for protein loading.

doxorubicin and TRAIL, PARP cleavage became evident (PARP in Fig. 8*C, Lanes 4, 8, 12,* and *16*).

Because there were no changes in the expression level of DR4, DR5, or FLIP after doxorubicin treatment in TRAIL-resistant cancer cell lines (data not shown), we investigated the effect of TRAIL or doxorubicin on the activation of caspases. In terms of doxorubicin sensitivity, TRAIL-resistant cancer cell lines can be divided into doxorubicin-sensitive (FADU) and doxorubicin-resistant (A875, J82, and SKOV3) cells (Fig. 8*C* and morphological data not shown).

In doxorubicin-sensitive FADU cells, caspase 8 was activated by doxorubicin treatment alone (caspase 8 in Fig. 8*C, Lane 7*). Caspase 9 was also activated by doxorubicin treatment alone in FADU cells (caspase 9 in Fig. 8*C, Lane 7*). Unexpectedly, however, although there was activation of caspases 8 and 9 ("initiator" caspases) in doxorubicin-treated FADU cells, we did not observe complete procaspase 3 ("executioner" caspase) depletion (caspase 3 in Fig. 8*C, Lane 7*). In the doxorubicin-resistant cell lines (A875, J832, and SKOV3), caspase activation was not observed after exposure to either doxorubicin alone or TRAIL alone (Fig. 8*C*). Interestingly, caspases 8, 9, and 3 became activated after exposure to the combination of doxorubicin and TRAIL (caspases 8, 9, and 3 in Fig. 8*C, Lanes 4, 12,* and *16*). In contrast to TRAIL-resistant cancer cells, cleavage of caspases 8, 9, and 3 was observed after TRAIL treatment of the TRAIL-sensitive HCT116 colon cancer cell line (Fig. 8*A*). When HCT116 was treated with TRAIL, PARP cleavage was evident by 4 h after TRAIL addition, and caspases 8, 9, 3, and 7 became activated at approximately the same time point (4 h after the TRAIL addition; Fig. 8*B*).

Discussion

The cytokine TRAIL is a promising agent for cancer therapy and is presently under investigation (6, 7). The importance of TRAIL as a potential anticancer agent is that it appears to be a potent cancer-specific cytotoxic drug and is not as toxic as other cytokines. TNF-α or Fas have not been successful in clinical trials when administered systemically because of toxicity (3, 4).

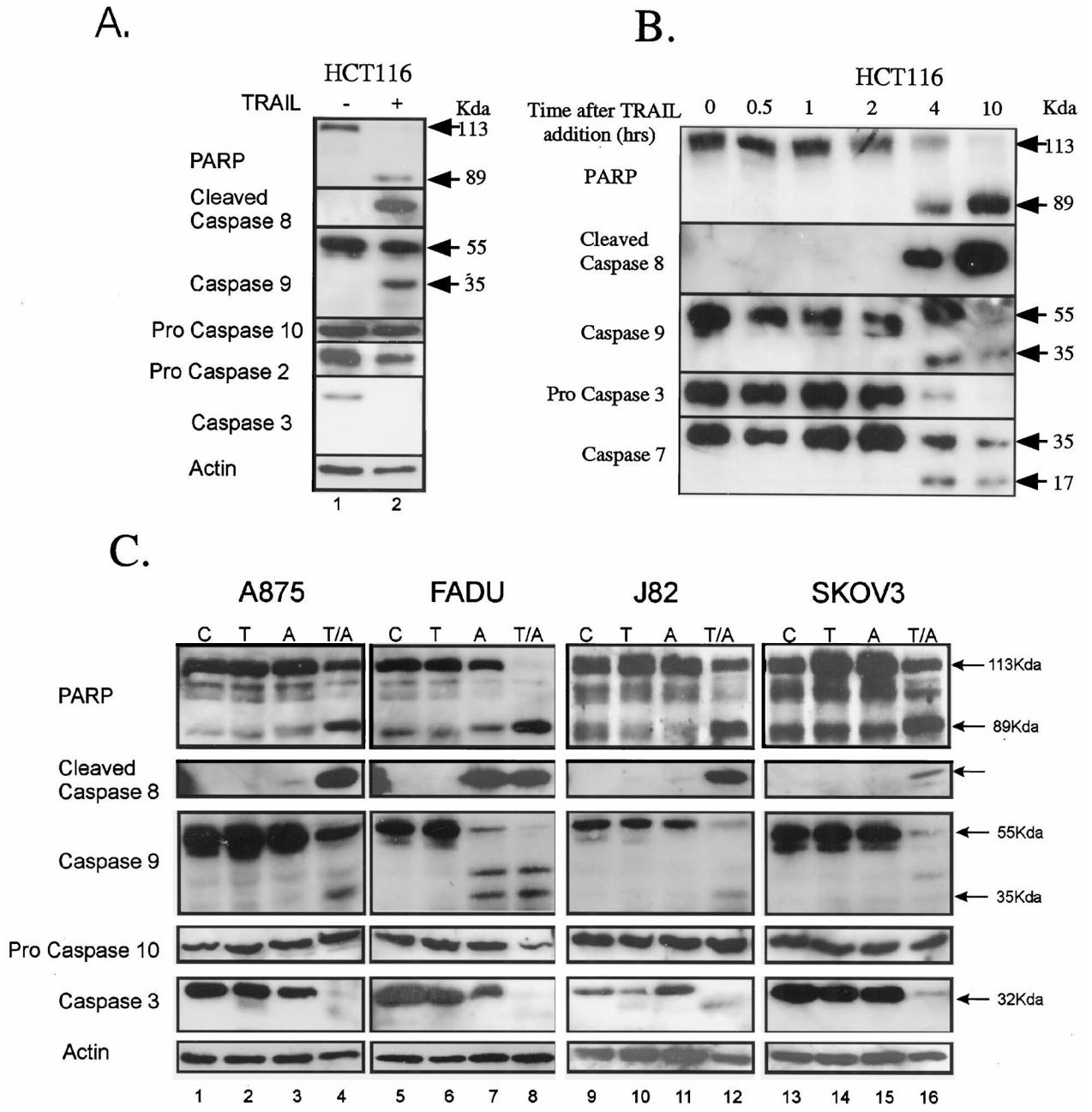

Fig. 8 Caspase activation after treatment by TRAIL alone or combined treatment using doxorubicin and TRAIL in TRAIL-sensitive and TRAIL-resistant cells. *A*, TRAIL-sensitive HCT116 cells were treated with TRAIL (200ng/ml) and cross-linked with the anti-FLAG M2 Ab (2 μg/ml). *B*, time course activation of caspases in HCT116 after treatment of TRAIL (200 ng/ml) cross-linked with anti-FLAG M2 Ab (2 μg/ml). Lysates were prepared at the indicated times shown above the figure. *C*, TRAIL-resistant cells were treated with TRAIL (200 ng/ml) cross-linked with the anti-FLAG M2 Ab (2 μg/ml) alone (*T*), doxorubicin (5 μM) alone (*A*), or with both (*T/A*) for 16 h. Cell lysates were prepared, and an equal amount of cellular protein was used for Western immunoblotting. *C* represents mock treatment.

Our results provide novel basic information relevant to TRAIL therapy of cancer in the following respects. First, we report that TRAIL resistance is mainly determined by the expression of its proapoptotic death receptors, especially DR4 ($r = 0.769$, $P = 0.006$). In fact, cell lines that were resistant to TRAIL were found to have a relatively low or undetectable expression level of DR4. Normal cell lines, such as HS27 and WI38, which are resistant to TRAIL, have extremely low expression of DR4 mRNA or protein (Fig. 2*B*, Fig. 3*A*, and Fig. 4), and a subgroup of TRAIL-resistant cells also have low or undetectable DR4 expression (Fig. 2*B* and Fig. 4). For DR4 expression alone, a χ^2 analysis revealed that this parameter is a

highly significant predictor of TRAIL sensitivity when expression is high *versus* low or undetectable ($P < 0.01$). For the χ^2 analysis, high expression was defined as DR4/GAPDH > 50 as shown in Fig. 2*C*. It is important to note that mRNA levels do not always correlate with protein levels and that the strength of the correlation between DR4 expression and TRAIL sensitivity (Fig. 2 and Fig. 3) might be stronger or weaker if the measured DR4 protein levels (Fig. 4) were actually quantitated. The expression of KILLER/DR5, however, does not correlate well with TRAIL sensitivity (Fig. 2 and Fig. 3*B*). Our observation is supported by a recent report that TRAIL sensitivity in melanoma cells correlates well with the expression level of DR4 (24). Contrary to our observation, J82 and SKOV3 expressed DR4 (Fig. 2*B* and Fig. 4) but were resistant to TRAIL treatment. A previous report that mutation in the death domain region of Fas can act as in a dominant-negative fashion in cell killing (25) prompted us to examine the death domain region of DR4 in J82 and SKOV3 cells. Indeed, J82 and SKOV3 have an A-to-G alteration at codon 441 in the death domain region of DR4 (Fig. 5*A*). However, that change is also found in 20% (2 of 10) of a normal population and thus, we refer to the DR4 K441R alteration as a polymorphism. Polymorphic DR4 acted in a dominant-negative manner in DR4-mediated cell killing (Fig. 6, *C* and *D*). We make no claim about any disease susceptibility associated with the K441R polymorphism in the DR4 gene. However, the presence of the K441R DR4 polymorphism in cancers may reduce their sensitivity to TRAIL, at least *in vitro.*

It is important to note the differences observed when full-length *versus* cytoplasmic domain expression constructs were used to express DR4. In particular, Fig. 6, *C* and *D* demonstrates that the cytoplasmic domain of DR4 does not itself induce cell death when it contains 441R. In addition, this variant of the cytoplasmic is capable of completely inhibiting death induced by the 441K allele. However, *full-length* DR4 containing the K441R mutation does not share these properties. Instead, full-length DR4 containing the 441R allele induces apoptosis in ~50% of transfected cells and poorly inhibits killing by the full-length 441K allele (Fig. 6*D, right*). These results suggest that the polymorphic 441R allele may contribute but cannot alone explain the observed resistance to TRAIL in certain cancer cell lines (J82 and SKOV3). These cell lines express somewhat increased levels of FLIP (Fig. 4), which may also contribute to their resistance to TRAIL (see below).

Second, the inhibitor of caspase activation FLIP may confer resistance to TRAIL at a point downstream of the death receptors. We found that 83% (five of six cell lines) of TRAIL-resistant cell lines showed a detectable expression of FLIP, whereas only one of five (20%) TRAIL-sensitive lines expressed FLIP (Fig. 4; χ^2; $P < 0.05$). However, the fact that FLIP-expressing PA1 cells are sensitive to TRAIL suggests that even in the presence of FLIP, cells can be killed if there is enough of an input signal for inducing apoptosis.

We measured the expression level of five genes (DR4, KILLER/DR5, TRID, TRUNDD, and FLIP) and tested for correlations with TRAIL sensitivity. The expression of two of the parameters (DR4 and FLIP) appeared to independently correlate with TRAIL sensitivity. From the regression analysis shown in Fig. 3, the *P* value for the DR4 correlation with TRAIL sensitivity is 0.006 (see legend of Fig. 3). Thus, we would have had to test 167 variables to reach the 0.006 level of significance at random for DR4 due to the effect of multiple testing. Moreover, the design of our study was hypothesis driven, with a biological basis giving a reasonable pretest probability of certain correlations. For example, we tested biologically plausible determinants of TRAIL sensitivity. One of the concerns with multiple correlations arises when one tests a very large number of variables (without a hypothesis), such as in a questionnaire with several hundred questions or perhaps a query of an expression of several thousand genes on a DNA microarray chip, and then develops the hypothesis based on any observed correlations at the $P < 0.05$ level. Of course, if one tests enough variables, there is a random chance that a few will appear to be significant but will actually be meaningless. Thus, because we believed that correcting for multiple testing artifacts would not significantly alter our *P*s or conclusions, we have not corrected our calculations for the effects of multiple comparisons. Thus, there is a small chance that our analysis may be limited by the effects of multiple comparisons, and it remains to be seen if others will find a similar significance of DR4 and FLIP expression levels using larger sample sizes and testing fewer variables.

Third, the targeted destruction of p53 to generate otherwise isogenic cancer cell lines revealed that TRAIL sensitivity could be modulated somewhat by p53 (Fig. 1). This is a preliminary observation that requires further investigation. It is clear from our data that wild-type p53 is not required for the apoptotic response to TRAIL.

Fourth, the combination of doxorubicin and TRAIL can kill TRAIL-resistant cancer cells, although each treatment alone cannot effectively kill the cells. The mechanism(s) of this additive killing is not clear yet. We have ruled out changes in the expression level of death receptors or FLIP as a basis for enhanced cell killing by doxorubicin plus TRAIL (data not shown). The fact that FADU cells show caspase 8 and 9 activation upon doxorubicin treatment suggests that the caspase activation axis from caspase 8 through Bcl2 inhibitory protein (Bid) to caspase 9 might be intact in FADU cells but not in other TRAIL-resistant cell lines (Fig. 8*C*). As recently reported (22) and observed in our experiments, doxorubicin and TRAIL could activate caspases in augmenting the killing effect. However, although TRAIL resistance can be overcome by combined treatment with doxorubicin, careful consideration should be given to the dose of doxorubicin given the observed sensitization of normal cells to TRAIL-mediated apoptosis (Fig. 7).

Fifth, among TRAIL-sensitive cancer cells, a certain fraction appears to be resistant to TRAIL-mediated killing (Fig. 1*B*). A recent report also showed that subclones of TRAIL-sensitive cancer cells display a variable response to TRAIL, although the expression level of TRAIL death receptors or FLIP was not changed (24). We do not know the underlying mechanism of this TRAIL resistance yet.

Our findings suggest that although TRAIL may be useful as a therapeutic agent in cancer, particular attention to molecular determinants of sensitivity needs to be considered to optimize such therapy. TRAIL does not appear to have harmful effects toward normal cells and can kill cancer cells irrespective of p53 status if wild-type DR4 is expressed on their cell surface. Our results also indicate that doxorubicin can sensitize cells to

TRAIL-mediated cell killing *in vitro*, thereby raising hopes that such a strategy may be useful in cancer therapy.

References

1. Wiley, S. R., Schooley, K., Smolak, P. J., Din, W. S., Huang, C. P., Nicholl, J. K., Sutherland, G. R., Smith, T. D., Rauch, C., and Smith, C. A. Identification and characterization of a new member of the TNF family that induces apoptosis. Immunity, *3:* 673–682, 1995.

2. Marsters, S. A., Pitti, R. M., Donahue, C. J., Ruppert, S., Bauer, K. D., and Ashkenazi, A. Activation of apoptosis by Apo-2 ligand is independent of FADD but blocked by CrmA. Curr. Biol., *6:* 750–752, 1996.

3. Nagata, S. Apoptosis by death factor. Cell, *88:* 355–365, 1997.

4. Schneider, P., Holler, N., Bodmer, J. L., Hahne, M., Frei, K., Fontana, A., and Tschopp, J. Conversion of membrane-bound Fas(CD95) ligand to its soluble form is associated with down-regulation of its proapoptotic activity and loss of liver toxicity. J. Exp. Med., *187:* 1205–1213, 1998.

5. Sheridan, J. P., Marsters, S. A., Pitti, R. M., Gurney, A., Skubatch, M., Baldwin, D., Ramakrishnan, L., Gray, C. L., Baker, K., Wood, W. I., Goddard, A. D., Godowski, P., and Ashkenazi, A. Control of TRAIL-induced apoptosis by a family of signaling and decoy receptors. Science (Washington DC), *277:* 818–821, 1997.

6. Walczak, H., Miller, R. E., Ariail, K., Gliniak, B., Griffith, T. S., Kubin, M., Chin, W., Jones, J., Woodward, A., Le, T., Smith, C., Smolak, P., Goodwin, R. G., Rauch, C. T., Schuh, J. C., and Lynch, D. H. Tumoricidal activity of tumor necrosis factor-related apoptosis-inducing ligand in vivo. Nat. Med., *5:* 157–163, 1999.

7. El-Deiry, W. S. The TRAIL to an anti-cancer agent. Drug Resistance Updates, *2:* 79–80, 1999.

8. Pan, G., O'Rourke, K., Chinnaiyan, A. M., Gentz, R., Ebner, R., Ni, J., and Dixit, V. M. The receptor for the cytotoxic ligand TRAIL. Science (Washington DC), *276:* 111–113, 1997.

9. Wu, G. S., Burns, T. F., McDonald, E. R., Jiang, W., Meng, R., Krantz, I. D., Kao, G., Gan, D. D., Zhou, J. Y., Muschel, R., Hamilton, S. R., Spinner, N. B., Markowitz, S., Wu, G., and El-Deiry, W. S. KILLER/DR5 is a DNA damage-inducible p53-regulated death receptor gene. Nat. Genet., *17:* 141–143, 1997.

10. Pan, G., Ni, J., Wei, Y. F., Yu, G., Gentz, R., and Dixit, V. M. An antagonist decoy receptor and a death domain-containing receptor for TRAIL. Science (Washington DC), *277:* 815–818, 1997.

11. Walczak, H., Degli-Esposti, M. A., Johnson, R. S., Smolak, P. J., Waugh, J. Y., Boiani, N., Timour, M. S., Gerhart, M. J., Schooley, K. A., Smith, C. A., Goodwin, R. G., and Rauch, C. T. TRAIL-R2: a novel apoptosis-mediating receptor for TRAIL. EMBO J., *16:* 5386–5397, 1997.

12. Screaton, G. R., Mongkolsapaya, J., Xu, X. N., Cowper, A. E., McMichael, A. J., and Bell, J. I. TRICK2, a new alternatively spliced receptor that transduces the cytotoxic signal from TRAIL. Curr. Biol., *7:* 693–696, 1997.

13. Degli-Esposti, M. A., Smolak, P. J., Walczak, H., Waugh, J., Huang, C. P., DuBose, R. F., Goodwin, R. G., and Smith, C. A. Cloning and characterization of TRAIL-R3, a novel member of the emerging TRAIL receptor family. J. Exp. Med., *186:* 1165–1170, 1997.

14. Mongkolsapaya, J., Cowper, A. E., Xu, X. N., Morris, G., McMichael, A. J., Bell, J. I., and Screaton, G. R. Lymphocyte inhibitor of TRAIL (TNF-related apoptosis-inducing ligand): a new receptor protecting lymphocytes from the death ligand TRAIL. J. Immunol., *160:* 3–6, 1998.

15. Pan, G., Ni, J., Yu, G., Wei, Y. F., and Dixit, V. M. TRUNDD, a new member of the TRAIL receptor family that antagonizes TRAIL signaling. FEBS Lett., *424:* 41–45, 1998.

16. Marsters, S. A., Sheridan, J. P., Pitti, R. M., Huang, A., Skubatch, M., Baldwin, D., Yuan, J., Gurney, A., Goddard, A. D., Godowski, P., and Ashkenazi, A. A novel receptor for Apo2L/TRAIL contains a truncated death domain. Curr. Biol., *7:* 1003–1006, 1997.

17. Degli-Esposti, M. A., Dougall, W. C., Smolak, P. J., Waugh, J. Y., Smith, C. A., and Goodwin, R. G. The novel receptor TRAIL-R4 induces NF-κB and protects against TRAIL-mediated apoptosis, yet retains an incomplete death domain. Immunity, *7:* 813–820, 1997.

18. Martinez-Lorenzo, M. J., Alava, M. A., Gamen, S., Kim, K. J., Chuntharapai, A., Pineiro, A., Naval, J., and Anel, A. Involvement of APO2 ligand/TRAIL in activation-induced death of Jurkat and human peripheral blood T cells. Eur. J. Immunol., *28:* 2714–2725, 1998.

19. Yeh, W. C., Pompa, J. L., McCurrach, M. E., Shu, H. B., Elia, A. J., Shahinian, A., Ng, M., Wakeham, A., Khoo, W., Mitchell, K., El-Deiry, W. S., Lowe, S. W., Goeddel, D. V., and Mak, T. W. FADD: essential for embryo development and signaling from some, but not all, inducers of apoptosis. Science (Washington DC), *279:* 1954–1958, 1998.

20. Zhang, J., Cado, D., Chen, A., Kabra, N. H., and Winoto, A. Fas-mediated apoptosis and activation-induced T-cell proliferation are defective in mice lacking FADD/Mort1. Nature (Lond.), *392:* 296–300, 1998.

21. Muhlenbeck, F., Haas, E., Schwenzer, R., Schubert, G., Grell, M., Smith, C., Scheurich, P., and Wajant, H. TRAIL/Apo2L activates c-Jun NH2-terminal kinase (JNK) via caspase-dependent and caspase-independent pathways. J. Biol. Chem., *273:* 33091–33098, 1998.

22. Keane, M. M., Ettenberg, S. A., Nau, M. M., Russell, E. K., and Lipkowitz, S. Chemotherapy augments TRAIL-induced apoptosis in breast cell lines. Cancer Res., *59:* 734–741, 1999.

23. Wang, J., Zheng, L., Lobito, A., Chan, F. K., Dale, J., Sneller, M., Yao, X., Puck, J. M., Straus, S. E., and Lenardo, M. J. Inherited human caspase 10 mutations underlie defective lymphocyte and dendritic cell apoptosis in autoimmune lymphoproliferative syndrome type II. Cell, *98:* 47–58, 1999.

24. Zhang, X. D., Franco, A., Myers, K., Gray, C., Nguyen, T., and Hersey, P. Relation of TNF-related apoptosis-inducing ligand (TRAIL) receptor and FLICE-inhibitory protein expression to TRAIL-induced apoptosis of melanoma. Cancer Res., *59:* 2747–2753, 1999.

25. Frank, S., Kohler, U., Schackert, G., and Schackert, H. K. Expression of TRAIL and its receptors in human brain tumors. Biochem. Biophys. Res. Commun., *257:* 454–459, 1999.

26. Rieger, J., Naumann, U., Glaser, T., Ashkenazi, A., and Weller, M. APO2 ligand: a novel lethal weapon against malignant glioma? FEBS Lett., *427:* 124–128, 1998.

27. Wu, G. S., and El-Deiry, W. S. Apoptotic death of tumor cells correlates with chemosensitivity, independent of p53 or Bcl-2. Clin. Cancer Res., *2:* 623–633, 1996.

28. Darzynkiewicz, Z., Li, X., and Gong, J. Assays of cell viability: discrimination of cells dying by apoptosis. Methods Cell. Biol., *41:* 15–38, 1994.

29. Chomczynski, P., and Sacchi, N. Single-step method of RNA isolation by acid guanidinium thiocyanate- phenol-chloroform extraction. Anal. Biochem., *162:* 156–159, 1987.

30. Prabhu, N. S., Somasundaram, K., Satyamoorthy, K., Herlyn, M., and El-Deiry, W. S. p73β, unlike p53, suppresses growth and induces apoptosis of human papillomavirus E6-expressing cancer cells. Int. J. Oncol., *13:* 5–9, 1998.

31. Pai, S. I., Wu, G. S., Ozoren, N., Wu, L., Jen, J., Sidransky, D., and El-Deiry, W. S. Rare loss-of-function mutation of a death receptor gene in head and neck cancer. Cancer Res., *58:* 3513–3518, 1998.

32. Meng, R. D., Shih, H., Prabhu, N. S., George, D. L., and El-Deiry, W. S. Bypass of abnormal MDM2 inhibition of p53-dependent growth suppression. Clin. Cancer Res., *4:* 251–259, 1998.

33. Griffith, T. S., Chin, W. A., Jackson, G. C., Lynch, D. H., and Kubin, M. Z. Intracellular regulation of TRAIL-induced apoptosis in human melanoma cells. J. Immunol., *161:* 2833–2840, 1998.

Analytical Biochemistry 394 (2009) 110–116

Contents lists available at ScienceDirect

Analytical Biochemistry

journal homepage: www.elsevier.com/locate/yabio

Identification of suitable reference genes for gene expression studies of human serous ovarian cancer by real-time polymerase chain reaction

Yan-Li Li [a], Feng Ye [a], Ying Hu [a], Wei-Guo Lu [b], Xing Xie [b,*]

[a] Women's Reproductive Health Laboratory of Zhejiang Province, Women's Hospital, School of Medicine, Zhejiang University, Xueshi Rd. No. 2, Hangzhou 310006, China
[b] Women's Reproductive Health Laboratory of Zhejiang Province, Department of Gynecologic Oncology, Women's Hospital, School of Medicine, Zhejiang University, Xueshi Rd. No. 2, Hangzhou 310006, China

ARTICLE INFO

Article history:
Received 8 June 2009
Available online 19 July 2009

Keywords:
Ovarian cancer
Real-time PCR
Reference gene
GeNorm
NormFinder

ABSTRACT

Quantitative real-time RT-PCR (RT-qPCR) has proven to be a valuable molecular technique in gene expression quantification. Target gene expression levels are usually normalized to a stably expressed reference gene simultaneously determined in the same sample. It is critical to select optimal reference genes to interpret data generated by RT-qPCR. However, no suitable reference genes have been identified in human ovarian cancer to date. In this study, 10 housekeeping genes, ACTB, ALAS1, GAPDH, GUSB, HPRT1, PBGD, PPIA, PUM1, RPL29, and TBP as well as 18S rRNA that were already used in various studies were analyzed to determine their applicability. Totally 20 serous ovarian cancer specimens and 20 normal ovarian epithelial tissue specimens were examined. All candidate reference genes showed significant differences in expression between malignant and nonmalignant groups except GUSB, PPIA, and TBP. The expression stability and suitability of the 11 genes were validated employing geNorm and NormFinder. GUSB, PPIA, and TBP were demonstrated as the most stable reference genes and thus could be used as reference genes for normalization in gene profiling studies of serous ovarian cancer, while the combination of two genes (GUSB and PPIA) or the all three genes should be recommended as a much more reliable normalization strategy.

Quantitative real-time reverse transcription-polymerase chain reaction (RT-qPCR)[1] has become an established and powerful technique for gene expression studies. Relative quantification is a crucial and frequently used method to assess RT-qPCR data, while target gene expression levels are associated with a stably expressed internal reference gene determined in the same biological sample at the same time. Identification of suitable reference genes is an important problem involved in this approach. The expression of an ideal reference gene should be stable, unregulated, and invariable under the conditions of experiment [1–3].

In the literature, the widely used reference genes include housekeeping genes, such as glyceraldehydes-3-phosphate dehydrogenase (GAPDH) and β-actin (ACTB) as well as ribosomal RNA (18S rRNA and 28S rRNA). However, some studies revealed that the expression levels of the commonly used reference genes did not always remain invariable; they varied across tissues [4] and cell types [5], as well as metabolic conditions and treatments [6]. Recently, some authors have discussed the identification of candidate reference genes for the relative quantification of expression data in cancers [7–10]. It has been suggested that all genes are regulated under some conditions and there is probably no universal reference gene with a constant expression in all tissues [11].

Ovarian cancer is the leading course of death from gynecological malignancy. An estimated 21,650 new cases of this malignancy were diagnosed and 15,520 deaths attributed to this disease in the United States during 2008 [12].The most frequent subtype of ovarian cancer is the serous subtype, which accounts for approximately 60 to 80% of ovarian cancer cases [13]. The majority of the patients (about 75%) are related to extraovarian spread at the time of diagnosis. The 5-year survival rate for women diagnosed with early-stage disease is approximately 95%, while survival rates drop to less than 30% when diagnosis is delayed until late stages. The condition has not been improved over the past few decades. In recent years, gene expression studies in malignant ovarian tissue and normal tissue counterpart have been performed to find new predictive and prognostic molecular markers associated with ovarian cancer. RT-qPCR is a frequently used tool to detect these markers. Thus, a scan on the normalization strategies used in quantitative gene expression studies of ovarian cancer is necessary. Combining the MeSH terms "ovarian cancer" and "real-time PCR," we performed a PubMed search of articles published from January 1, 2004 to

* Corresponding author. Fax: +86 571 87036290.
E-mail address: xiex@mail.hz.zj.cn (X. Xie).

[1] *Abbreviation used*: RT-qPCR, quantitative real-time reverse transcription-polymerase chain reaction.

0003-2697/$ - see front matter © 2009 Elsevier Inc. All rights reserved.
doi:10.1016/j.ab.2009.07.022

May 1, 2009 and got 119 available articles that use 21 various reference genes. Surprisingly, only 11 (9.2%) out of 119 studies used multiple reference genes for data normalization. Within the other 108 (90.8%) studies that applied a single reference gene, GAPDH was the most frequently used normalizer (52 times, 43.7%), followed by ACTB (23 times, 19.3%) and 18S rRNA (11 times, 9.2%). Apart from the three genes, all the other cited genes accounted for only 0.8 to 3.4%, such as HPRT1, GUSB, RPL29, PBGD, and TBP. Moreover, housekeeping genes and rRNAs were used as reference genes without any preliminary evaluation of suitability. The search results also clearly reveal that a systematic study on the selection of appropriate reference genes for gene expression studies in ovarian cancer has not been carried out until now and it is urgent to perform a specific evaluation of the currently used reference genes.

Therefore, the goal of our study was to identify the most suitable gene or set of genes as reference genes in gene expression studies of ovarian cancer. In the current study, we validated the stability of a panel of 11 putative reference genes in ovarian cancer tissues and normal ovarian epithelial tissues, each from 20 patients. The 11 candidate genes are commonly used as endogenous controls in the context of, but not restricted to, ovarian cancer: ACTB, ALAS1, GAPDH, TBP, HPRT1, RPL29, PBGD, PPIA, PUM1, GUSB, and 18S rRNA. Some of them have been identified as optimal reference genes in some other cancer types, such as TBP [14] and HPRT1 [3].We were able to evaluate gene expression stability between ovarian cancer and normal ovarian epithelium employing geNorm software [15,16] and NormFinder [11,17].

Materials and methods

Patients and samples

Primary tumor samples ($n = 20$) were obtained from untreated ovarian cancer patients (mean age 56 years, range 39–71 years; 5 premenopausal and 15 postmenopausal) underwent tumor resection surgery. Normal ovarian epithelial tissue samples ($n = 20$) were derived from postmenopausal women who required bilateral adnexectomy when undergoing surgery because of other gynecological diseases (uterine prolapse, hysteromyoma, endometrial polyps, and ovarian simple cyst). All tumors were primary serous ovarian carcinoma. Histological analysis of H&E-stained sections showed that all cancer samples contained at least 90% tumor cells without necrosis. All the normal ovarian samples were verified to be free of any pathology. Tumor stage and grade were determined according to the International Federation of Gynecology and Obstetrics standards (FIGO). One of the 20 tumors was classified as stage I, 5 tumors stage II, 11 tumors stage III, and two tumors stage IV. The histological grading was one G1, 4 G2, and 15 G3. All of the specimens were collected at the Women's Hospital, School of Medicine, Zhejiang University, China. After excision, specimens were immediately snap-frozen in liquid nitrogen within about half an hour and stored at −80 °C until RNA extraction. Informed consent was obtained from each woman, and the study received the approval of the Ethical Committee for Clinical Research of Women's Hospital, School of Medicine, Zhejiang University.

RNA extraction and cDNA synthesis

Preserved tissue samples (50–100 mg) were homogenized in 1 ml TRIzol reagent (Invitrogen, Carlsbad, CA, USA) using a bench-top homogenizer (Polytron PT1600E, Kinematica AG, LittauLuzem, Switzerland) and total RNA was isolated from homogenized tissues according to the manufacturer's protocol. An additional step of RNase-free DNase I ((TaKaRa Biotechnology, Japan) treatment was performed. Concentrations of the isolated RNA and the 260/280 absorbance ratio were measured with a Nanodrop ND-1000 spectrophotometer (Nanodrop Technologies, DE, USA). The integrity of RNA samples was confirmed by electrophoresis on a 1% agarose gel. The criterion to include RNA samples was $260/280 \approx 2$ (1.9 to 2.2) and 28S/18S ratio $\geqslant 1.7$. The concentration of RNA was adjusted to 0.5 μg/μl with nuclease-free water. One microgram total RNA was reverse-transcribed to cDNA using a PrimeScript RT reagent kit (perfect real-time) (TaKaRa Biotechnology, Japan) in a total volume of 20 μl according to the manufacturer's instructions. The kit uses PrimeScript RTase, which is based on reverse transcriptase originated from M-MLV, and offers a fast, complete, and high-yield cDNA synthesis for real-time PCR. Briefly, RNA samples, buffer, RNase free water, enzyme mix, random 6 mers, and oligo (dT) were mixed and incubated for 15 min at 37 °C, followed by 5 s at 85 °C to inactivate enzymes. Primer complementary DNA was stored at −80 °C until use.

Real-time quantitative PCR

Eleven putative reference genes were selected for investigation to identify the most stable reference gene that could be used for normalization in RT-qPCR studies of ovarian cancer: ACTB, ALAS1, GAPDH, TBP, HPRT1, RPL29, PBGD, PPIA, PUM1, GUSB, and 18S rRNA (Table 1). They belong to different abundance and functional classes. Oligonucleotide primers were designed with primer5 software according to the sequences obtained from GeneBank database (Table 2). All primers except for 18S rRNA spanned at least one intron to minimize inaccuracies due to genomic DNA contamination in RNA samples. The specificity of the primer sequences were confirmed by BLAST searches. SYBR green real-time PCR was performed with an Applied Biosystems 7900HT Fast Real-time PCR system using the SYBR Premix Ex Taq (perfect real time) (TaKaRa Biotechnology).The PCR volume was 20 μl, containing 1 μl cDNA. The following cycling conditions were used [95 °C for 10 s, (95 °C for 10 s, 60 °C or 63 °C for 30 s) × 40 cycles]. All reactions were run in duplicate and all 40 samples were analyzed in the same run in order to exclude between-run variations. No tem-

Table 1
Putative reference genes evaluated.

Gene symbol	GeneBank Accession No.	Gene name	Genomic localization	Molecular function
18S	NR_003286	18S ribosomal RNA	22p12	Ribosome subunit
ACTB	NM_001101	Beta-actin	7p15–p12	Cytoskeletal structural protein
ALAS1	NM_000688	Aminolevulinate, delta-, synthase 1	3p21.1	5-Aminolevulinate synthase
GAPDH	NM_002046	Glyceraldehyde-3-phosphate dehydrogenase	12p13	Oxidoreductase in glycolysis and gluconeogenesis
GUSB	NM_000181	Beta-glucuronidase	7q21.11	Galactosidase
HPRT1	NM_000194	Hypoxanthine phosphoribosyltransferase 1	Xq26	Metabolic salvage of purines
PBGD	NM_000190	Porphobilinogendeaminase	11q23	Hydroxymethylbilane synthase
PPIA	NM_021130	Peptidylprolyl isomerase A	7p13	Cyclosporin binding protein
PUM1	NM_001020658	Pumilio homolog 1 (Drosophila)	1p35.2	RNA binding
RPL29	NM_000992	Ribosomal protein L29	3p21.3–p21.2	Structural constituent of ribosome
TBP	NM_003194	TATA box binding protein	6q27	General transcription factor

Table 2
Details of primers and amplicons for the 11 evaluated genes.

Gene	Forward primer sequence[5′ → 3′]	Genomic position	Reverse primer sequence[5′ → 3′]	Genomic position	Amplicon length
18S	CGGCTACCACATCCAAGGAA	1st Exon	GCTGGAATTACCGCGGCT	1stExon	186 bp
ACTB	AGAAAATCTGGCACCACACC	3rd Exon	TAGCACAGCCTGGATAGCAA	4th Exon	173 bp
ALAS1	GGCAGCACAGATGAATCAGA	4th Exon	CCTCCATCGGTTTTCACACT	5th Exon	150 bp
GAPDH	GACAGTCAGCCGCATCTTCT	1st Exon	TTAAAAGCAGCCCTGGTGAC	3rd Exon	127 bp
GUSB	AGCCAGTTCCTCATCAATGG	6th Exon	GGTAGTGGCTGGTACGGAAA	7th Exon	160 bp
HPRT1	GACCAGTCAACAGGGGACAT	4th Exon	CCTGACCAAGGAAAGCAAAG	6th Exon	132 bp
PBGD	AGTGTGGTGGGAACCAGC	9th Exon	CAGGATGATGGCACTGAACTC	10, 11th Exon	144 bp
PPIA	AGACAAGGTCCCAAAGAC	2nd Exon	ACCACCCTGACACATAAA	4th Exon	118 bp
PUM1	CAGGCTGCCTACCAACTCAT	16th Exon	GTTCCCGAACCATCTCATTC	17, 18th Exon	211 bp
RPL29	GGCGTTGTTGACCCTATTTC	1st Exon	GTGTGTGGTGTGGTTCTTGG	2nd Exon	120 bp
TBP	TGCACAGGAGCCAAGAGTGAA	4th Exon	CACATCACAGCTCCCCACCA	5th Exon	132 bp

plate controls (no cDNA in PCR) were included in each assay run for each gene. A melting curve was constructed for each primer pair to confirm product specificity.

Threshold cycles (C_t values), the cycle number at which the fluorescence signal of the sample exceeds background fluorescence, were determined for quantitative comparison of the amplification of the candidate genes. C_t values were transformed to relative quantities for analysis considering the PCR efficiencies of the candidate reference genes according to the equation, $E^{(\text{minCt}-\text{sampleCt})}$, in which min$C_t$ = lowest C_t value over a range of samples for a given primer pair and E = amplification efficiency (2 = 100%) [16].

PCR efficiency

A 10-fold dilution series was created from a random pool of cDNA from our sample groups ranging from ×1 dilution to ×100,000 dilutions. PCR were performed as described above in triplicate. The PCR efficiency and correlation coefficients (R^2) of each primer pair were generated using the slops of the standard curves. The efficiencies were calculated by the formula: efficiency (%) = $(10^{(-1/\text{slope})} - 1) * 100$.

Date analysis

Statistical analyses were performed with SPSS 15.0 program. The distribution fitting procedure according to the D'Agostino–Pearson omnibus normality test and Student's *t*-tests were applied. Since type II error is uncontrollable in a two-sided *t*-test, we also performed an equivalence test suggested by Haller et al. [18]: whether the difference of the expected logarithmized expression level δ is bounded by a determined number ε is concerned in this test. The hypothesis is defined as H_0: $\delta \notin [-\varepsilon; \varepsilon]$ versus H_1: $\delta \in [-\varepsilon; \varepsilon]$. If the confidence interval (CI) for the difference δ of the expected logarithmized expression values is included by the determined deviation area, a candidate reference gene can be considered as equivalent in expression on level α. The analyst constructs a $100(1-2\alpha)\%$ confidence level (CI) for the difference between the two mean values of two groups and compares it with the determined deviation area, $[-\varepsilon; \varepsilon]$. If the CI for the difference of the expected logarithmized expression values in two groups is completely contained within the interval $[-\varepsilon; \varepsilon]$, candidate reference genes can be considered as equivalent in expression on level α. The lower border and the upper border of the CI can be calculated according to the formula [18]

$$\text{CI}(\delta) = [\delta\text{L}; \delta\text{H}], \tag{1}$$

$$\delta_{\text{L,U}} = (\overline{X}_1 - \overline{X}_2) \mp S\sqrt{\frac{1}{N_1} + \frac{1}{N_2}} \times t_{1-\alpha,N_1+N_2-2} \tag{2}$$

$$S = \sqrt{\frac{(N_1-1)\times S_1^2 + (N_2-1)\times S_2^2}{N_1+N_2-2}} \tag{3}$$

In which S_1 and S_2 are the standard deviation of the logarithmized expression values in groups 1 and 2; N_1 and N_2 are the number of samples in the two groups; $t_{1-\alpha,N_1+N_2-2}$means $1-\alpha$ quantile of the t distribution with N_1+N_2-2 degrees of freedom. As noted above, if $[\delta_L; \delta_H] \in [-\varepsilon; \varepsilon]$, H_0 could be rejected. In addition, $[\delta_L; \delta_H]$ must contain 0.

Correlations between gene expression level (a continuous scale variable) and tumor stage and FIGO stage as well as menopausal status were characterized by the Spearman's rank test. Association between gene expression and patient age was assessed applying Pearson's test. A constant level $\alpha = 0.05$ were used for rejection of null hypothesis in all statistical tests. $P < 0.05$ was considered statistically significant.

For stability comparisons of candidate reference genes, the software geNorm, version 3.5, and NormFinder programs were applied according to the recommendations. The program geNorm is available on the internet http://medgen.ugent.be/genorm/. It calculates the expression stability measure (M) for candidate reference genes and by stepwise exclusion of the gene with highest M value in each step allows ranking of the tested genes according to their expression stability. It also provides a way to determine how many reference genes were needed for accurate normalization. NormFinder is a Microsoft Excel add-in and calculates a stability value for each individual candidate reference gene and ranks the genes according to their expression stability value in certain samples derived from a designed experiment [11]. The stability value is based on the combined estimate of intra- and intergroup variation of gene expression. A low stability value indicates a low combined variation and reveals high expression stability. Employing NormFinder, a best combination of two reference genes is also calculated.

Results

Quality control

To avoid erroneous conclusions, only RNA samples with high quality were included in this study. The selected RNA samples isolated from 20 malignant and 20 nonmalignant specimens all exhibited a high quality. The mean $A_{260/280}$ ratio of the RNA samples was 2.01 ± 0.045 (range from 1.95 to 2.12) and reflected pure and protein-free RNA. The integrity of RNA samples was characterized by the 28S/18S ratio (>1.7) on a 1% agarose gels.

The amplification efficiencies and correlation coefficients (R^2) of the 11 candidate genes were generated using the slopes of the standard curves obtained by serial dilutions. Correlation coefficients (R^2) ranged from 0.995 to 0.999 and PCR efficiencies from 98 to 108% (Supplementary Fig. 1). The amplification specificity for each qRT-PCR analysis was confirmed by melting curve analysis (Supplementary Fig. 2). Furthermore, PCR products were separated by 1.5% agarose gel to confirm an expected single band at the right amplicon size.

Expression levels of candidate reference genes

The 11 candidate reference genes displayed a wide expression range, with C_t values between 9.54 and 33.03. All genes showed a normal distribution pattern proved by the D'Agostino–Pearson fitting procedure in both the malignant and the nonmalignant tissue samples. As shown in Fig. 1, the nonmalignant and the malignant samples were separately shown as box plots with ranges as whiskers to demonstrate the total expression ranges. Among these genes, 18S rRNA is the most abundant transcript with mean (±SD) C_t values of 10.67 ± 0.9 in malignant and 11.33 ± 0.85 in nonmalignant samples. PBGD is the lowest expressed gene with mean (±SD) C_t values of 26.83 ± 1.2 in malignant and 29.98 ± 2.2 in nonmalignant samples. Significant differences in gene expression between malignant and nonmalignant samples were observed for all candidate reference genes, except GUSB ($P = 0.121$), PPIA ($P = 0.27$), and TBP ($P = 0.49$). Interestingly, compared with nonmalignant samples, the expressions of 18S rRNA, ACTB, ALAS1, GAPDH, HPRT1, PUM1, and RPL29 were all significantly increased in malignant samples with a very low P value ($P < 0.001$).

We used a fold change of 3 in equivalence test as suggested by Haller et al. [18]. Thus, the $[-\varepsilon; \varepsilon] = [\log_2 1/3; \log_2 3] = [-1.58496, 1.58496]$. The CI ($\delta$) values for GUSB, PPIA, and TBP were [−0.11283; 1.11183], [−0.17239; 1.35239], and [−0.36503; 0.87403], respectively, which were completely contained within [−1.58496, 1.58496] and contain 0. Thus, the expressions of GUSB, PPIA, and TBP are equivalent in the tumor and control groups. The CI (δ) value for 18S, [0.09086; 1.23634], was part of the determined deviation area but did not contain 0 and thus the null hypothesis could not be rejected. The CI (δ) values for ACTB [2.19612; 3.88787], ALAS1 [2.30874; 3.66726], GAPDH [3.27525; 4.87175], HPRT1 [0.58475; 2.46525], PBGD [2.15847; 4.13653], PUM1 [1.68741; 3.26359] and RPL29 [2.99850; 4.18250] were not bounded by the determined deviation area, and therefore the eight candidate reference genes were not equivalently expressed in the two groups. Hence, the possibility of a type II error (false negatives) in the t-test was excluded and the results were further confirmed through this approach.

Additionally, the expression of these candidate genes did not depend on age (correlation coefficient = −0.111 to 0.345; $P = 0.136$ to 1.000), menopausal status (correlation coefficient = −0.132 to 0.208; $P = 0.379$ to 1.000), FIGO stage (correlation coefficient = −0.336 to 0.203; $P = 0.147$ to 0.922), and tumor degree (correlation coefficient = −0.093 to 0.255; $P = 0.279$ to 0.977).

Expression stability of candidate reference genes

Including the 3 suitable genes, all 11 candidate reference genes were included in the program geNorm and ranked according to their M values (Fig. 2a). The M value is the average pairwise variation of an individual gene with all other control genes. The M values for GUSB, PPIA, TBP, 18S rRNA, HPRT1, PUM1, RPL29, ALAS1, and ACTB were lower than the geNorm default threshold of 1.5, while the two remaining genes, GAPDH and RPL29, showed M values greater than the threshold. GUSB and PPIA (both $M = 0.842$) were identified as the two most stable genes according to geNorm analysis. After excluding the 8 genes noted that differ in expression between groups, the geNorm analysis was repeated. The most stable genes were still PPIA and GUSB, followed by TBP, which was in accord with the previous finding. To determine the optimal number of genes required for RT-qPCR date normalization, geNorm calculates the pairwise variation ($Vn/Vn + 1$) between sequential normalization factors (NF) (NFn and NF$n + 1$). A large variation means that the added gene has a significant effect and should preferably be included for calculation of a reliable normalization factor [16]. As shown in Fig. 2b, the pairwise variation (v) on normalization with the three most stable reference genes, PPIA, GUSB, and TBP, and introduction of the fourth one was 0.188. The trend of the value became roughly stable after the addition of the eighth gene.

To compare the result generated from geNorm, another free tool available on the internet to validate the expression stability was also used. The stability data calculated by that program was a combined estimate of intra- and intergroup expression variations of the genes studied. It could reveal the expression differences of the genes observed between normal and tumor groups. The result of the analysis by NormFinder appeared to be similar to the one determined by geNorm (Table 3). The three genes GUSB, PPIA, and 18S rRNA achieved the best stability values, and the best combination of two genes was that of GUSB and PPIA.

Discussion

It is well recognized that the reference gene should be properly validated for a particular experiment to ensure that gene expres-

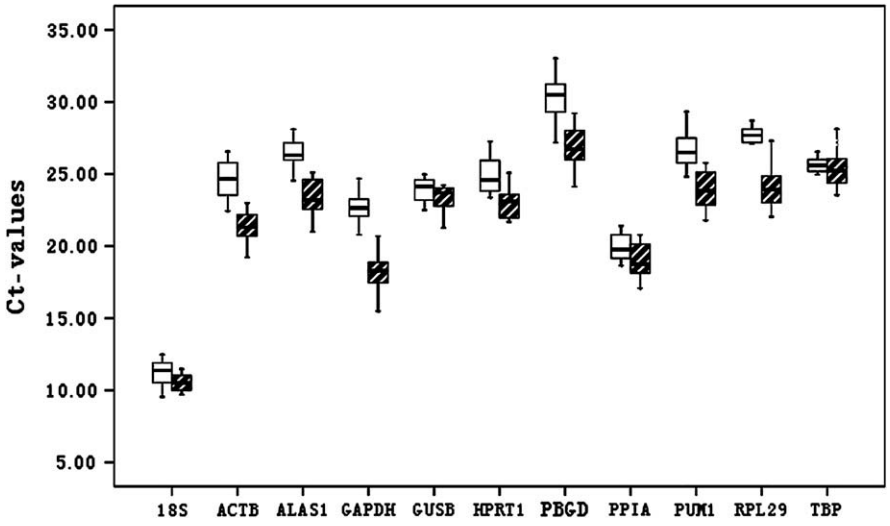

Fig. 1. Expression levels of candidate reference genes in normal ovarian epithelia and serous ovarian cancer samples. Values are given as real-time PCR cycle threshold numbers (C_t values). Boxes (blank, normal; cross-striated, cancer) represent the lower and upper quartiles with medians; whiskers represent the ranges for the data of the 20 samples in each group.

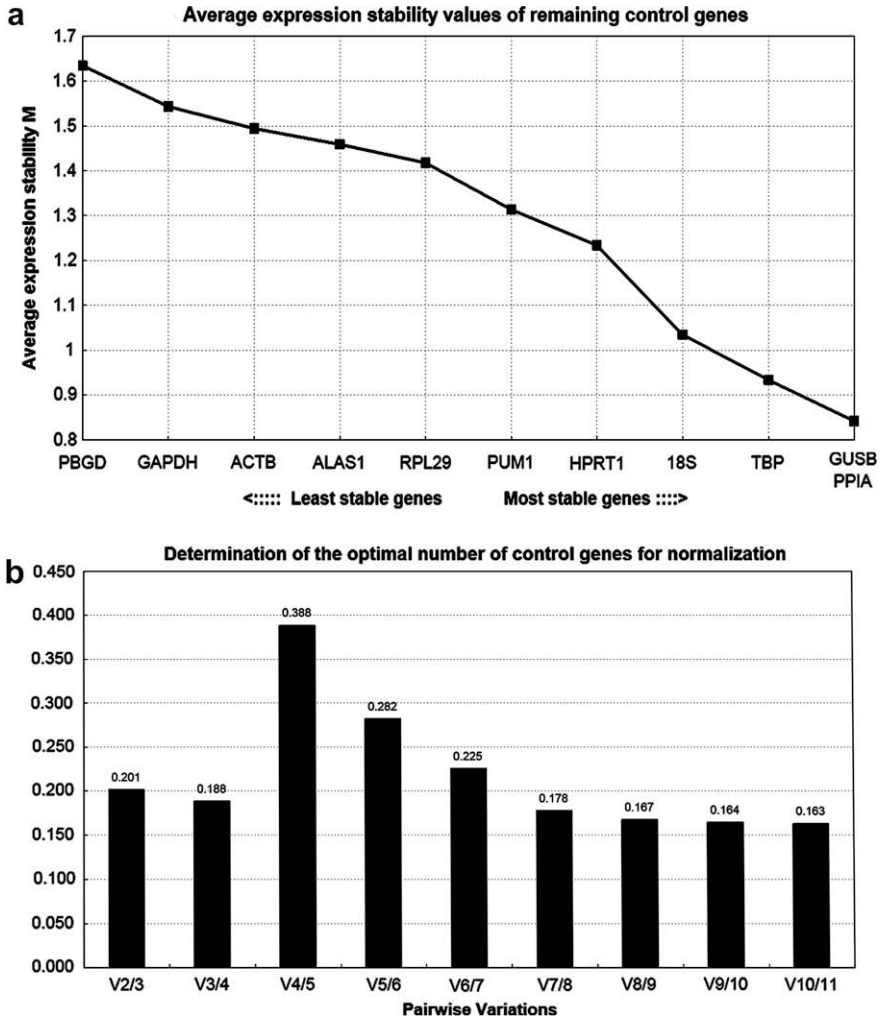

Fig. 2. GeNorm analysis of the candidate reference genes. Results are presented according to the output file of the geNorm program. (a) Stepwise exclusion of the least stable genes by calculating the average expression stability measure *M*. The value of *M* was calculated for each gene, and the least stable gene with the highest *M* value was automatically excluded for the next calculation round. The *x*-axis from left to right indicates the ranking of the reference genes according to expression stability and the *y*-axis indicates the stability measure, *M*. (b) Determination of the optimal number of reference genes for normalization.

Table 3
Candidate reference genes for normalization listed according to their expression stability calculated by the NormFinder program.

Raking order	Gene name	Stability value
1	PPIA	0.338
2	GUSB	0.345
3	18S	0.401
4	TBP	0.492
5	PUM1	0.633
6	ALAS1	0.795
7	ACTB	0.839
8	PBGD	0.906
9	RPL29	0.950
10	GAPDH	1.160
11	HPRT1	5.226

sion is unaffected by the experimental treatment. As far as we are aware, there are no published articles about optimal reference gene selection for ovarian cancer. We report herein the first systematic comparison of expression stability of candidate reference genes in ovarian carcinoma samples and benign counterparts.

A group of widely used reference genes have been applied in recent ovarian cancer gene profiling studies, such as GAPDH, ACTB, TBP, 18S rRNA, RPL29, GUSB, and HPRT1, for RT-PCR [19–24]. In the present study, we evaluated a panel of 11 candidate reference genes to determine the most reliable one for accurate normalization of gene expression.

To obtain reliable data, we carefully designed our study before RT-qPCR analysis based on the following features: (1) The majority of patients with ovarian cancer are diagnosed at late stages, when the whole ovary has been damaged and it is difficult to get tumor tissues and valid paratumor tissues in the same ovary. Thus, we obtained normal ovarian epithelial tissues from patients receiving surgery because of benign gynecological diseases, though it is known that the use of paired samples from the same patient may minimize the interindividual variation [3,8]. (2) We used strict RNA quality control, precise RNA concentration determination, and gene-specific primer selection, (3) simultaneous examination of a considerable number of 11 candidate genes from different function classes, and (4) employment of two received software, geNorm and NormFinder, combined with a *t*-test and a equivalence test to rank the candidate reference genes according to their stability.

The expression of candidate reference genes can be influenced not only by tissue types but also by physiological or pathological factors like age, tumor stage, and tumor grade. Thus, it should be decided whether the expression is correlated with the biological

conditions listed above. The results of our data proved that the expression of these genes in this cohort was independent on age, FIGO stage, and tumor grade. Additionally, because ovarian epithelial tissues obtained from postmenopausal women were used as normal control, we also evaluated the correlation between candidate gene expression and menopausal status. The results showed there was no association between the two variables and thus the use of a control group described above was warranted and feasible. However, due to the reduced size of the cohort of patients in this study, a definite correlation between gene expression and clinic pathologic features should be further determined in a larger sample.

In the current study, we calculated the best performing reference genes using two distinct statistical models, a pairwise comparison model, geNorm, and an ANOVA-based model, NormFinder. Finally, geNorm identified GUSB, PPIA, and TBP as the three most stably expressed reference genes while NormFinder indicated GUSB, PPIA, and 18S rRNA as the three genes with the best stability, followed by TBP. However, the previously performed *t*-test and equivalence test analyses of gene expression in malignant and nonmalignant groups revealed that only three genes GUSB, PPIA, and TBP did not differ in their expression in the two groups. It could be concluded only the three genes fulfill the criterion of expression stability and could be considered as suitable normalizers for relative gene quantification in serous ovarian cancer samples. Thus, 18s RNA should be excluded and GUSB, PPIA, and TBP were finally indicated as the three most stable reference genes for studying target gene profiling in serous ovarian cancer.

However, it is recommended that normalization using a single reference gene should be replaced by normalization based on the several best performing candidate reference genes [15]. A normalization strategy applying multiple reference genes has the benefit of minimizing the influence of minor fluctuations and making accurate data normalization is also suggested by some other authors [25,26]. In the present study, we found GUSB, PPIA, and TBP yield a variation value of 0.188. As reported by Vandesompele et al. [16], though GeNorm proposes a pairwise variation of 0.15 as the cutoff under which the inclusion of an additional reference gene is unnecessary, the cutoff of 0.15 should not be considered in a strict sense, but rather as guidance to determine the optimal number of reference genes. Sometimes the observed trend can be equally informative, and using the three best reference genes is, in most cases, a valid normalization strategy. Therefore, GUSB, PPIA, and TBP is a reliable set of genes for normalizing data generated from RT-qPCR analysis in serous ovarian cancer. Additionally, GUSB and PPIA were also indicated as the best combination of two genes by NormFinder.

Nevertheless, as a limitation of our study, we should note that the present study is limited to the serous ovarian cancer subtype. However, it is the most frequent subtype of ovarian carcinoma. The applicability of the three recommended reference genes GUSB, PPIA, and TBP in other subtypes of ovarian cancer was not tested and further studies are needed to confirm their potential use.

In conclusion, our current study demonstrated that the three most stable genes GUSB, PPIA, and TBP could be used as reference genes for normalization in gene profiling studies of serous ovarian cancer and the combination of two genes (GUSB and PPIA) or the all three genes should be recommended as a much more reliable normalization strategy.

Acknowledgments

We appreciate financial support from the National Natural Science Foundation of China (No. 30672230 and No. 30672229).

Appendix A. Supplementary data

Supplementary data associated with this article can be found, in the online version, at doi:10.1016/j.ab.2009.07.022.

References

[1] O. Thellin, W. Zorzi, B. Lakaye, B.B. De Borman, B. Coumans, G. Hennen, T. Grisar, A. Igout, E. Heinen, Housekeeping genes as internal standards: use and limits, J. Biotechnol. 75 (1999) 291–295.
[2] A. Radonic, S. Thulke, I.M. Mackay, O. Landt, W. Siegert, A. Nitsche, Guideline to reference gene selection for quantitative real-time PCR, Biochem. Biophys. Res. Commun. 313 (2004) 856–862.
[3] F. Ohl, M. Jung, C. Xu, C. Stephan, A. Rabien, M. Burkhardt, A. Nitsche, G. Kristiansen, A. Radonic, K. Jung, Gene expression studies in prostate cancer tissue: which reference gene should be selected?, J Mol. Med. 83 (2005) 1014–1024.
[4] N.R. Mansur, K. Meyer-Stegler, J.C. Wurtz, M.A. Sirover, Cell cycle regulation of the glyceraldehydes-3-phosphate dehydrogenase/uracil glycosylase gene in normal human cell, Nucleic Acids Res. 21 (1993) 993–998.
[5] J. Blomberg, M. Andersson, R. Faldt, Differential pattern of oncogene and beta-actin expression in leukaemic cells from AML patients, Br. J. Haematol. 65 (1987) 83–86.
[6] T.D. Schmittgen, B.A. Zakrajsek, Effect of experimental treatment on housekeeping gene expression: validation by real-time, quantitative RT-PCR, J. Biochem. Biophys. Methods 46 (2000) 69–81.
[7] M. Jung, A. Ramankulov, J. Roigas, M. Johannsen, M. Ringsdorf, G. Kristiansen, K. Jung, In search of suitable reference genes for gene expression studies of human renal cell carcinoma by real-time PCR, BMC Mol. Biol. 8 (2007) 47.
[8] V.R. Cicinnati, Q. Shen, G.C. Sotiropoulos, A. Radtke, G. Gerken, S. Beckebaum, Validation of putative reference genes for gene expression studies in human hepatocellular carcinoma using real-time quantitative RT-PCR, BMC Cancer 8 (2008) 350.
[9] S. Saviozzi, F. Cordero, M. Lo Iacono, S. Novello, G.V. Scagliotti, R.A. Calogero, Selection of suitable reference genes for accurate normalization of gene expression profile studies in non-small cell lung cancer, BMC Cancer 6 (2006) 200.
[10] C.L. Andersen, J.L. Jensen, T.F. Orntoft, Normalization of real time quantitative reverse transcription-PCR data: a model based variance estimation approach to identify genes suited for normalization, applied to bladder and colon cancer data sets, Cancer Res. 64 (2004) 5245–5250.
[11] M. Kubista, J.M. Andrade, M. Bengtsson, A. Forootan, J. Jonak, K. Lind, R. Sindelka, R. Sjoback, B. Sjogreen, L. Strombom, A. Stahlberg, N. Zoric, The real-time polymerase chain reaction, Mol. Aspects Med. 27 (2006) 95–125.
[12] A. Jemal, R. Siegel, E. Ward, Y. Hao, J. Xu, T. Murray, M.J. Thun, Cancer statistics 2008, CA Cancer J. Clin. 58 (2008) 71–96.
[13] K. Levanon, C. Crum, R. Drapkin, New insights into the pathogenesis of serous ovarian cancer and its clinical impact, J. Clin. Oncol. 26 (2008) 5284–5293.
[14] J.B. de Kok, R.W. Roelofs, B.A. Giesendorf, J.L. Pennings, E.T. Waas, T. Feuth, D.W. Swinkels, P.N. Span, Normalization of gene expression measurements in tumor tissues: comparison of 13 endogenous control genes, Lab. Invest. 85 (2005) 154–159.
[15] J. Vandesompele, K. De Preter, F. Pattyn, B. Poppe, N. Van Roy, A. De Paepe, Accurate normalization of real-time quantitative RT-PCR data by geometric averaging of multiple internal control genes, Genome Biol. 3 (2002) RESEARCH0034. research0034.1–research0034.11.
[16] J. Vandesompele, K. De Preter, F. Pattyn, B. Poppe, N. Van Roy, A. De Paepe, F. Speleman, GeNorm software manual, update 6 2004. Available from: <http://medgen.ugent.be/~jvdesomp/genorm>.
[17] NormFinder Software. Available from: <http://www.mdl.dk/publicationsnormfinder.htm>.
[18] F. Haller, B. Kulle, S. Schwaqer, B. Gunawan, A. von Heydebreck, H. Sültmann, L. Füzesi, Equivalence test in quantitative reverse transcription polymerase chain reaction: confirmation of reference genes suitable for normalization, Anal. Biochem. 335 (2004) 1–9.
[19] F.W. Wamunyokoli, T. Bonome, J.Y. Lee, C.M. Feltmate, W.R. Welch, M. Radonovich, C. Pise-Masison, J. Brady, K. Hao, R.S. Berkowitz, S. Mok, M.J. Birrer, Expression profiling of mucinous tumors of the ovary identifies genes of clinicopathologic importance, Clin. Cancer Res. 12 (2006) 690–700.
[20] K.Y. Chan, H. Ozçelik, A.N. Cheung, H.Y. Ngan, U.S. Khoo, Epigenetic factors controlling the BRCA1 and BRCA2 genes in sporadic ovarian cancer, Cancer Res. 62 (2002) 4151–4156.
[21] M.E. Urick, P.A. Johnson, Cyclooxygenase 1 and 2 mRNA and protein expression in the Gallus domesticus model of ovarian cancer, Gynecol. Oncol. 103 (2006) 673–678.
[22] N. Eckstein, K. Servan, B. Hildebrandt, A. Pölitz, G. Von Jonquières, S. Wolf-Kümmeth, I. Napierski, A. Hamacher, M.U. Kassack, J. Budczies, M. Beier, M. Dietel, B. Royer-Pokora, C. Denkert, H.D. Royer, Hyperactivation of the insulin-like growth factor receptor I signaling pathway is an essential event for cisplatin resistance of ovarian cancer cells, Cancer Res. 69 (2009) 2996–3003.
[23] A. Potapova, A.M. Hoffman, A. Godwin, K.T. Al-Saleem, P. Cairns, Promoter hypermethylation of the PALB2 susceptibility gene in inherited and sporadic breast and ovarian cancer, Cancer Res. 68 (2008) 998–1002.

[24] S. Cunat, F. Rabenoelina, J.P. Daur'es, D. Katsaros, H. Sasano, W.R. Miller, T. Maudelonde, P. Pujol, Aromatase expression in ovarian epithelial cancers, J. Steroid Biochem. Mol. Biol. 93 (2005) 15–24.
[25] C. Tricarico, P. Pinzani, S. Bianchi, M. Paglierani, V. Distante, M. Pazzagli, S.A. Bustin, C. Orlando, Quantitative real time reverse transcription polymerase chain reaction: normalization to rRNA or single housekeeping genes is inappropriate for human tissue biopsies, Anal. Biochem. 309 (2002) 293–300.
[26] H. Schmid, C.D. Cohen, A. Henger, S. Irrgang, D. Schlondorff, M. Kretzler, Validation of endogenous controls for gene expression analysis in microdissected human renal biopsies, Kidney Int. 64 (2003) 356–360.

Alinhamentos

Iniciadores descritos por Kim et al 2000

```
>KILLER/DR5F
GGGAGCCGCTCATGAGGAAGTTGG

> KILLER/DR5R
GGCAAGTCTCTCTCCCAGCGTCTC

CLUSTAL O(1.2.4) multiple sequence alignment


SEQ1             GGGAGCCGCTCATGAGGAAGTTG-  23
KILLER/DR5F      GGGAGCCGCTCATGAGGAAGTTGG  24
                 ***********************
#
#
#  Percent Identity  Matrix - created by Clustal2.1
#
#

     1: SEQ1         100.00  100.00
     2: KILLER/DR5F  100.00  100.00


CLUSTAL O(1.2.4) multiple sequence alignment


SEQ2             GGCAAGTCTCTCTCCCAGCGTCTC  24
KILLER/DR5R      GGCAAGTCTCTCTCCCAGCGTCTC  24
                 ************************
#
#
#  Percent Identity  Matrix - created by Clustal2.1
#
#

     1: SEQ2         100.00  100.00
     2: KILLER/DR5R  100.00  100.00
```

Iniciadores descritos por li et al 2009

```
>TBPf
TGCACAGGAGCCAAGAGTGAA

>TBPR
CACATCACAGCTCCCCACCA


CLUSTAL O(1.2.4) multiple sequence alignment


3          TGCACAGGAGCCAAGAGTGAA   21
TBPf       TGCACAGGAGCCAAGAGTGAA   21
           ********************
#
#
#  Percent Identity  Matrix - created by Clustal2.1
```

```
#
#

     1: 3           100.00  100.00
     2: TBPf        100.00  100.00


CLUSTAL O(1.2.4) multiple sequence alignment


4         CACATCACAGCTCCCCACCA    20
TBPR      CACATCACAGCTCCCCACCA    20
          ********************
#
#
#  Percent Identity  Matrix - created by Clustal2.1
#
#

     1: 4           100.00  100.00
     2: TBPR        100.00  100.00
```